






Review

# Fused Deposition Modelling of Polymer Composite: A Progress

J Mogan <sup>1</sup>, W. S. W. Harun <sup>2,\*</sup>, K. Kadirgama <sup>3</sup>, D. Ramasamy <sup>2</sup>, F. M. Foudzi <sup>4</sup>, A. B. Sulong <sup>4</sup>,  
F. Tarlochan <sup>5</sup> and F. Ahmad <sup>6</sup><sup>1</sup> Institute of Postgraduate Studies, Universiti Malaysia Pahang, Gambang, Kuantan 26300, Pahang, Malaysia<sup>2</sup> Department of Mechanical Engineering, College of Engineering, Universiti Malaysia Pahang, Gambang, Kuantan 26300, Pahang, Malaysia<sup>3</sup> Faculty of Mechanical and Automotive Engineering Technology, Universiti Malaysia Pahang, Gambang, Kuantan 26300, Pahang, Malaysia<sup>4</sup> Department of Mechanical and Manufacturing Engineering, Faculty of Engineering and Built Environment, Universiti Kebangsaan Malaysia, Bangi 43600, Selangor, Malaysia<sup>5</sup> Department of Mechanical and Industrial Engineering, College of Engineering, Qatar University, Doha P.O. Box 2713, Qatar<sup>6</sup> Department of Mechanical Engineering, Universiti Teknologi Petronas, Seri Iskandar 32610, Perak, Malaysia

\* Correspondence: sharuzi@ump.edu.my

**Abstract:** Additive manufacturing (AM) highlights developing complex and efficient parts for various uses. Fused deposition modelling (FDM) is the most frequent fabrication procedure used to make polymer products. Although it is widely used, due to its low characteristics, such as weak mechanical properties and poor surface, the types of polymer material that may be produced are limited, affecting the structural applications of FDM. Therefore, the FDM process utilises the polymer composition to produce a better physical product. The review's objective is to systematically document all critical information on FDMed-polymer composite processing, specifically for part fabrication. The review covers the published works on the FDMed-polymer composite from 2011 to 2021 based on our systematic literature review of more than 150 high-impact related research articles. The base and filler material used, and the process parameters including layer height, nozzle temperature, bed temperature, and screw type are also discussed in this review. FDM is utilised in various biomedical, automotive, and other manufacturing industries. This study is expected to be one of the essential pit-stops for future related works in the FDMed-polymeric composite study.

**Keywords:** FDM; polymer; composite; properties; process parameter; application



**Citation:** Mogan, J.; Harun, W.S.W.; Kadirgama, K.; Ramasamy, D.; Foudzi, F.M.; Sulong, A.B.; Tarlochan, F.; Ahmad, F. Fused Deposition Modelling of Polymer Composite: A Progress. *Polymers* **2023**, *15*, 28. <https://doi.org/10.3390/polym15010028>

Academic Editor: Ali Bagheri

Received: 18 October 2022

Revised: 4 November 2022

Accepted: 10 November 2022

Published: 21 December 2022



**Copyright:** © 2022 by the authors. Licensee MDPI, Basel, Switzerland. This article is an open access article distributed under the terms and conditions of the Creative Commons Attribution (CC BY) license (<https://creativecommons.org/licenses/by/4.0/>).

## 1. Introduction

Manufacturing industries are rapidly evolving in terms of the technology and materials involved. AM has transformed the industries of affordable three-dimensional (3D) solid structure fabrication and rapidly converting computer-generated designs into actual parts [1,2]. In recent years, AM has emerged as one of the most effective processes where the material is printed layer-upon-layer for building 3D products. Rapid prototyping, rapid manufacturing, and 3D printing are terms used to describe AM, which is snowballing in the manufacturing sector because the product can be served directly to the consumers, resulting in lower capital expenditure and transportation costs. Furthermore, AM fabricates customised parts in small quantities, which do not need special tools and allow the fabrication of complex geometries and assemblies [3,4]. In addition, 3D printing technology has advanced rapidly in recent years, and now various field applications are available, such as industries in the biomedical [5,6], aerospace [7,8], and automotive fields [9]. Unlike the traditional manufacturing processes [10], 3D printing is an AM method that works by stacking material from one layer over another to produce complex structures [11].

Metals, polymers, and composites can be used in AM. Many applications use AM technologies to create a complex shape [12]. There are many AM processes, such as selective

laser sintering (SLS) [13], fused deposition modelling (FDM) [14], direct metal deposition (DMD) [15], laminated object manufacturing (LOM) [16], ink jet modelling (IJM) [17], and stereo-lithography (SLA) [18]. These procedures differ in printing material, process parameters, precision level, and end-use application [19]. FDM, also known as fused filament fabrication (FFF), is very well used in 3D printing. Stratasys Inc. in the United States invented the method during the 1990s. Printing factors such as printing orientation, air gap, layer thickness, raster width, and raster angle can be adjusted to improve the quality of printed parts [20]. Although FDM is known for its low operating cost and low investment cost, the printed products are more fragile as compared to other standard plastic manufacturing methods, such as moulding, injection [21], CNC [22], and extrusion [23,24].

Composites are materials of two or more physically or chemically separate phases divided by a discrete interface. The different elements are deliberately merged to produce a system with much more effective structural and functional properties than any of the constituents could achieve on their own [25].

Whether natural or synthetic, polymer composites are amongst the most significant applications of polymer. In various polymer matrices, the polymer composite is a multi-phase solid substance in which one phase has at least 1, 2, or 3 dimensions. The polymer composites are viable for use as a high-performance composite when the reinforcing properties differ significantly from or exceed that matrix. The polymer matrix composite is the most enhanced composite material; these composite materials have various classifications of fibres such as natural and synthetic fibres as the reinforced materials in various types of polymer, for instance, thermoplastic polymer or thermoset polymer, which can be moulded into various shapes and sizes to produce various types of antiquated material [26].

By applying the feeding force created by the grooved bearing and driving gear, material in the form of a filament is fed into the liquefier head over the spool, as shown in Figure 1. The thermoplastic filament is heated to a glass transition temperature before being deposited in layers using a heated nozzle. The head of the liquefier travels through the X-Y plane according to the tool path supplied by programming. Support material can be eliminated with a solvent after fabrication [27].

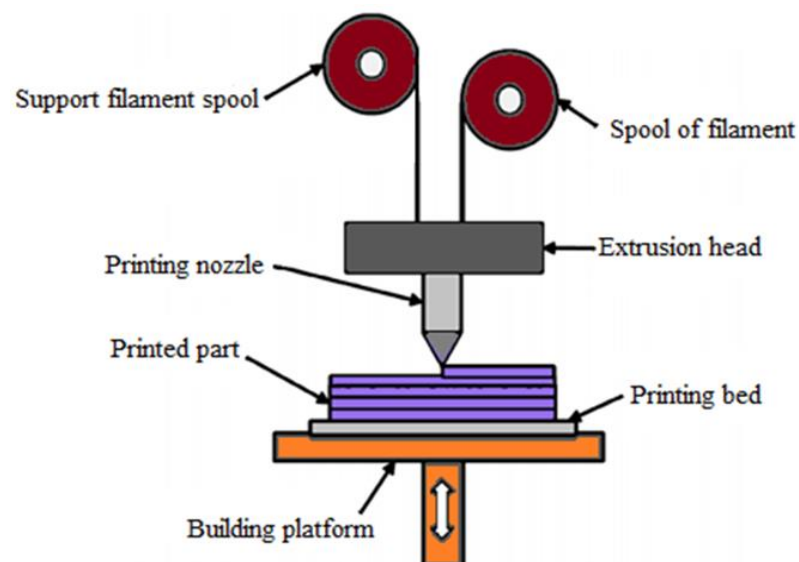
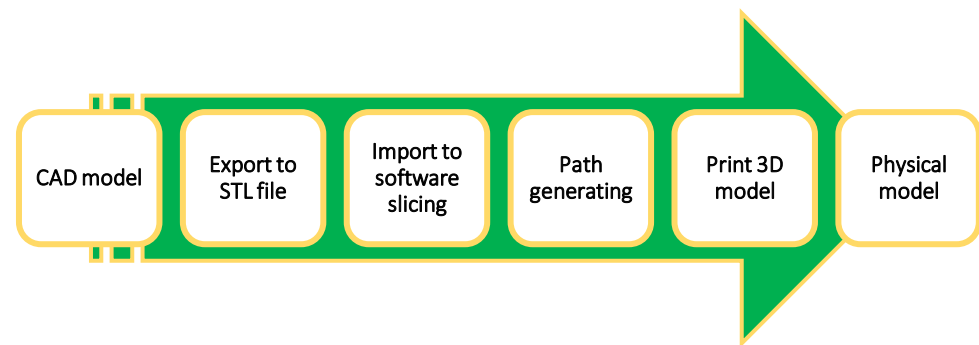


Figure 1. Schematic diagram of FDM process.

Figure 2 shows the steps involved in the FDM process. The process begins with designing a digital model of a part by using CAD software. Then, 3D scanning, and reverse engineering are also performed to create a digital model. Later, the digital model is converted into a Standard Tessellation Language or Standard Triangle Language (STL) file. The STL file contains data about the surface geometry of the model. Then, the STL file is

fed into the slicer software after conversion. Slicing determines the condition of printed pieces. Next, they apply information from the STL file, and the slicer generates G-codes. The generated G-code is the same as the CNC machine. It also controls the extruder and platform's direction during printing. After converting the G-codes from an STL file, the 3D printer is ready to print a physical object of the design. This printing differs regardless of the kind of AM technique used. In the FDM process, the nozzle follows the G-code instructions and moves to deposit the melted filament in layers. The G-code controls the amount of material extruded, movement of the extruder nozzle, and extrusion time. After the whole model is printed, some post-processing is required to ensure a satisfactory product finish [28].



**Figure 2.** Steps involved in the FDM process to produce 3D printed parts.

Even though the FDM process generates high-quality machinable materials, the world currently requires far more effective 3D printed parts than the traditional approaches, which can be gained by combining polymer with other materials, such as carbon, ceramic, metal, and many others, which are known as polymer composites. This review paper discusses the polymer composite using the FDM process from 2011 to 2021. As for this review paper, around 150 high-impact related research articles have been analysed to obtain the related information by using a research matrix table method. The paper also discusses polymer composite utilisation in the FDM process and its properties, as well as processing parameters and applications of the FDM process used in various industries. The dimensional accuracy of FDM-printed prototypes is one of the many aspects that determine the performance of fabricated prototypes because it influences the outcome of further prototype investigations. In addition, many printing parameters such as extrusion temperature, layer thickness, printing speed, raster width, and infill pattern are proven to significantly impact dimensional accuracy [29].

## 2. Composite Materials

Composite materials have developed into engineering materials that are remarkable and diverse because they are strong in domain areas that do not deform easily and have a high strength-to-weight ratio [30,31]. A composite material is defined by its name, which implies that it is made of different materials. Compositional engineering occurs when many constituent materials with significantly different chemical or/and physical properties are combined to form a new material with unique characteristics that are not present in the individual element [32–37]. Compared to the qualities of individual materials, this augmentation makes composite materials preferable. There are different types of composite material: scale base composite, reinforced base composite, matrix material base composite, and bio-composite. Figure 3 summarises the types of composite material. A composite material comprises two materials, namely base and filler. Because it wraps and bonds the reinforcement of other materials, the base material is commonly known as a matrix or a binder material. Fibres, particles, fragments, and natural or synthetic whiskers are filler materials [38–40]. Matrix is a soft phase with mechanical and physical properties, such as formability, ductility, and thermal conductivity. Material with high stiffness, strength, and

low thermal fluctuation is included in the matrix reinforcement. The reinforcement phase of composites is always stiffer and more robust than the matrix because it conveys the load applied to the material.

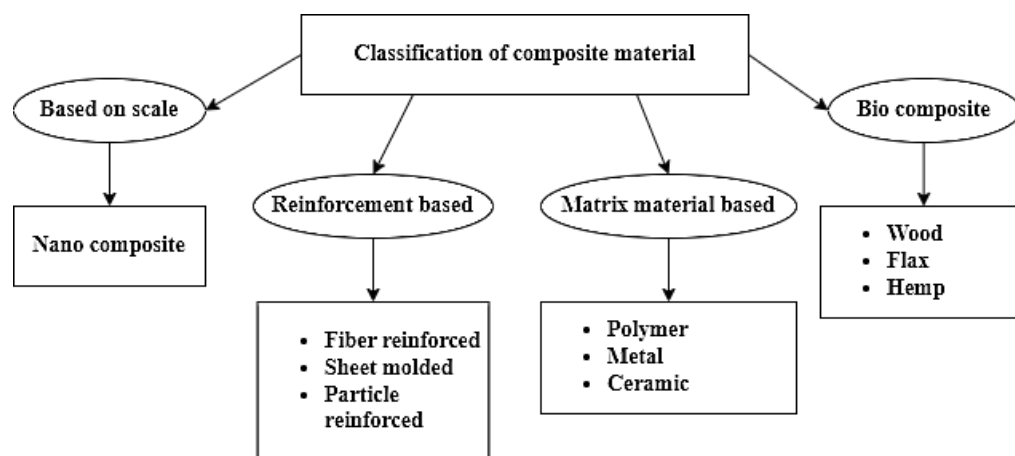


**Figure 3.** Detailed classification of composite materials.

### 2.1. Polymer Matrix Composite

A polymer matrix composite (PMC) is a composite material consisting of a natural polymer grid that holds a series of smaller uniform filaments. PMCs are designed to transport loads between matrix material filaments. PMCs are composed of a thermosetting or thermoplastic matrix with carbon, Kevlar, glass, and metal fibres dispersed throughout [41–44]. Thermosets are more commonly used than thermoplastics because of their increased strength and tolerance to high temperatures [45]. Thermosets are made by combining resins that are hardened together. The most common type of laminar structure is created by stacking and bonding thin layers of fibre and polymer until the appropriate thickness is achieved. Due to facile handling procedures and cheap manufacturing methods, PMCs are inexpensive composites [46,47]. Polymers can be utilised as the base matrix. Metals, generally in powders, are often used as the reinforcement, resulting in a material with unique qualities. The PMC has proliferated in recent years due to the demand for additional innovative engineering materials with higher strength and lower weight [48,49]. Figure 4 explains the classification of matrix composites. There are three types of matrix composites: metal matrix composites (MMC), ceramic matrix composites (CMC), and polymer matrix composites (PMC).

### 2.2. Base Material

AM and eventually the fabrication of original equipment manufacturer (OEM) components rely heavily on polymer materials. There are two kinds of thermoplastic materials in use today, which are thermoplastic and thermoplastic composites. The use of large-capacity polymer thermosets and elastomer materials in AM is a relatively new technique. FDM technology uses a variety of thermoplastics as feedstocks, including acrylonitrile butadiene styrene (ABS), polylactic acid (PLA), polycarbonate (PC), polyether ether ketone (PEEK), polyethylene terephthalate glycol (PETG), and nylon [50,51]. Table 1 shows thermoplastics used in FDM process.

Figure 5 shows the base materials used in the FDM process. The most used base material is ABS, and the second most used is PLA. Both are thermoplastic materials that are commonly used materials in the FDM process. Comparatively, materials other than ABS and PLA are used at a minimum, at no more than 10%. PC, PEEK, and PETG are thermoplastics primarily utilised in engineering applications. ABS is a popular thermoplastic material for the FDM process because ABS has excellent melt fluidity, strength, and stiffness.

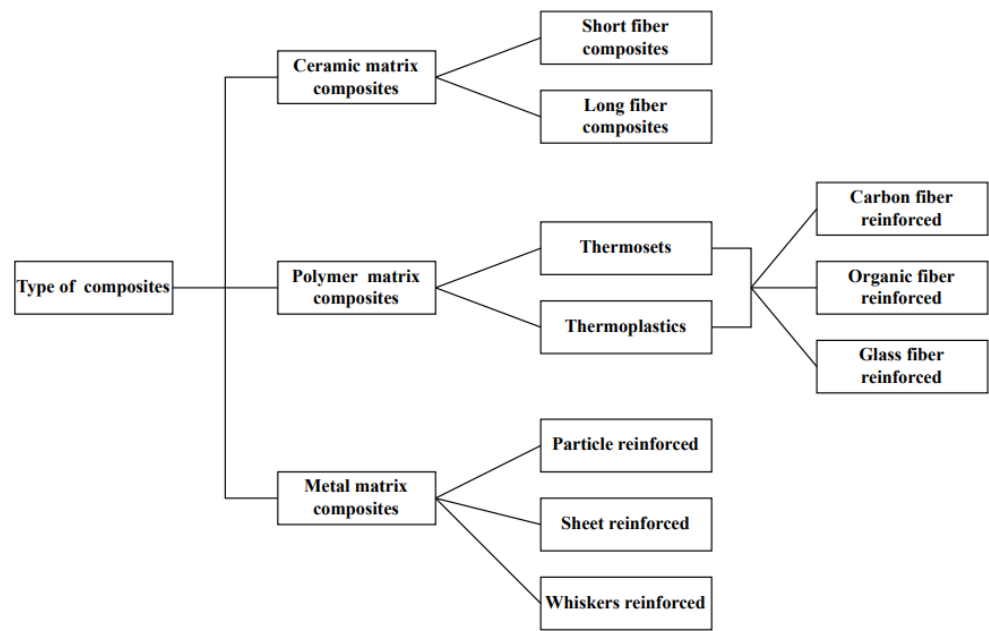


Figure 4. Classification of the type of matrix composites.

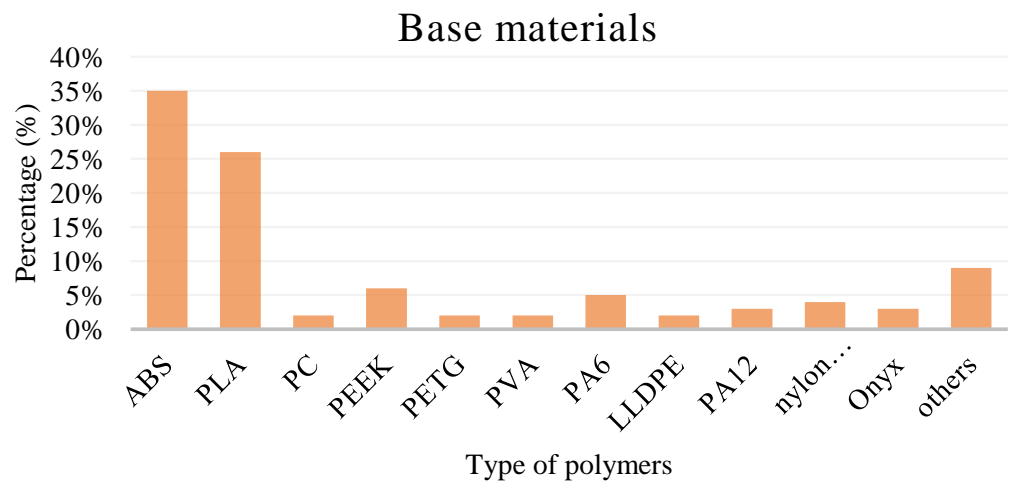


Figure 5. Type of polymer used as a base material in the FDM process.

FDM ABS products’ impact and tensile properties are poor compared to injection-moulded components [52]. FDM-manufactured ABS products have a 34% lower tensile strength than injection-moulded products. PLA is another popular thermoplastic material utilised in the FDM process because of its biodegradable qualities and wide range of uses in the medical sector. PLA has low ductility as compared to ABS. However, it has high strength. During the printing of the PLA composite, a rise in void content and anisotropy is observed, similar to ABS composites in the FDM process [53].

### 2.3. Filler Material

Plastics can be reinforced with a variety of fillers, including metals and numerous organic compounds from plants, to create composites. These fillers can be used to increase a composite’s characteristics, surface appeal, sustainability, or cost. Figure 6 shows filler materials used in the FDM process based on polymer composite-related published work. Carbon is the most used filler material (39%). The commonly used carbons are carbon nanotubes, graphite, graphene, and carbon black. There are a few carbon nanotubes: single-walled carbon nanotubes (SWNT) and multi-walled carbon nanotubes (MWCNTs).

SWNTs are cylindrical graphitic tubules with diameters of approximately 1.0 nm. MWCNTs are a unique structure of carbon nanotubes, whereby the multiple single-walled carbon nanotubes are enclosed inside each other. Fibres can be classified into two categories: natural fibre and synthetic fibre. The natural fibre is extracted from animals, cellulose, and minerals. Fibre from minerals is asbestos. Animal fibres are silk, hair, and wool.

**Table 1.** Thermoplastic used in FDM process.

References	Type of Materials	Characterisation	Utilisation Sector	Remarks
[54–58]	Acrylonitrile butadiene styrene (ABS)	Better resistance to corrosive materials Low cost Withstand high temperature	Microdevices Microfluidics Prototyping  Tissue engineering	Dissolves in acetone
[59–65]	Polylactic Acid (PLA)	Low cost Non-toxic Biodegradable Ease to print	Automotive Electrical and Electromagnetic Biomedical Biosensors Prototyping	Very brittle Low toughness
[66–68]	Polyamide/Nylon	Resistant to impact Heat-resistant High tensile strength Transparent	Fabrication tools Prototyping Industrial production parts	Moisture accumulation
[69–72]	Polycarbonate (PC)	Temperature-resistant High resistance to impact	Dental Tissue engineering Orthopaedic	
[73,74]	Thermoplastic polyurethane (TPU)	Good lubricity Abrasion-resistant	Hoses and tubes Biomedical prototype Seals and gaskets	Elastomeric behaviour
[24,75–78]	Polyether-ether-ketone (PEEK)	Organic thermoplastic polymer Chemical-resistant Good lubricity	Aircraft parts Racing cars Drones Medical implants	
[79–82]	Polyethene terephthalate glycol (PETG)	Chemical-resistant Transparent High processability	Bone models Orthopaedics	Become brittle due to heat
[59,64]	Polyvinyl alcohol (PVA)	Soluble in water	Dental models Bioprinting Brackets	Affected by humidity
[83,84]	Polyetherimide (PEI)	Chemical-resistant Heat-resistant Dielectric	Aerospace Automotive Medical	Better than conventional plastic products

In contrast, cellulose is usually extracted from bast, leaf fruit, wood, seed, grass, and stalk. There are two divisions of synthetic fibre: organic fibre and inorganic fibre. Organic fibre consists of polyethene, aromatic polyester, and aramid fibre. Inorganic fibres are glass, boron, carbon, and silica carbide [26]. Although there is much information about continuous fibre-reinforced thermoplastic composites, there is not much on chopped carbon fibre-reinforced thermoplastic composites. This employs the FDM process to create composites and explore the impact of chopped carbon fibre on the thermo-mechanical properties of PLA composites [27]. Table 2 shows the filler materials in FDM process to enhance properties of polymer.



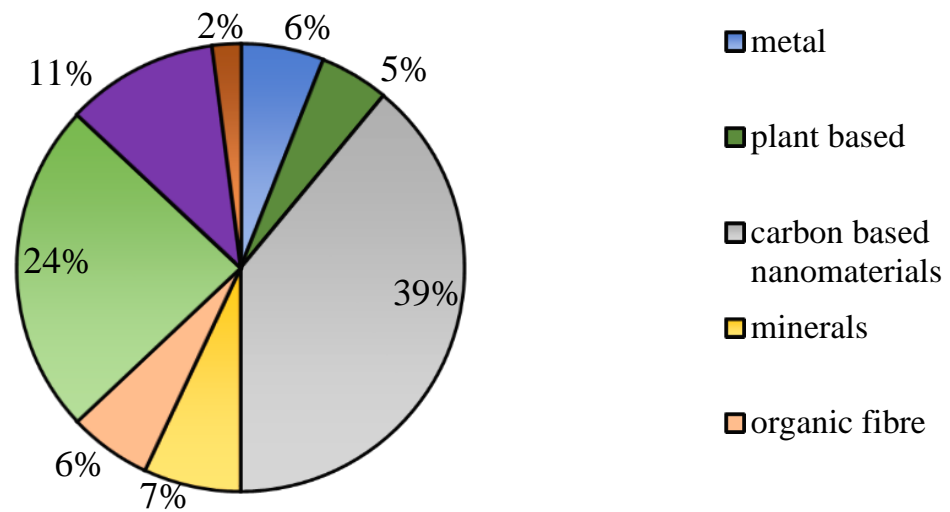


Figure 6. Materials that are used as filler to enhance properties of polymer.

Table 2. Classification of filler material and the conducted test.

Classification	Filler Material	Type of Base Material Used	Composition (wt%)	Test	Reference
Metal	Aluminium	PLA	6.95	Tensile	[85–87]
	Copper	PLA	4, 8, 12, 16, 20	Compression and flexural	[88–90]
	Stainless steel	-	-	Density measurement	[91]
Plant-based	Cork	PLA	5, 10, 15, 20, 25, 30, 50	Tensile and density measurement	[92,93]
	Wood particle	PLA	30, 40	Tensile, flexural	[94–96]
	Cellulose	PLA	1, 2, 5, 10, 20	Tensile, flexural	[97–100]
Carbon-based nanomaterials	Carbon black	ABS	3, 1.5	Density measurement, tensile	[101,102]
		PLA	5, 53	-	[103–105]
	Graphene	ABS	2, 4, 6, 8	Tensile, flexural, impact, hardness	[106–109]
		PC/ABS ABS/EPDM	0.2, 0.4, 0.6, 0.8 2, 4, 6, 8, 10	Tensile -	[110,111] [112]
	Carbon nanotubes	ABS	1, 3, 5, 7, 10	Tensile, density measurement	[101,113,114]
		PLA	10	Electrical conductivity	[115,116]
Mineral	Hydroxyapatite (HA)	PLA	5, 10, 15	Compression and flexural	[117,118]
		PCL	10, 20	Compression and tensile	[119–121]
		PEEK	10, 20, 30, 40	Tensile	[122]
Organic fibre	Kenaf bast fibre	PCL	5, 10, 20	Tensile and flexural	[123]
	Aramid fibre	Nylon polymer	2	Surface roughness	[124]
	Flax fibre	PLA	-	Tensile	[125]

Table 2. Cont.

Classification	Filler Material	Type of Base Material Used	Composition (wt%)	Test	Reference
Inorganic fibre	Carbon fibre	ABS	1, 2, 3, 5, 7.5, 10, 15	Tensile, flexural, surface roughness, dimensional accuracy	[126–128]
		PLA	12, 15, 20	Tensile, compression, flexural, hardness, impact	[129–132]
		PEEK	10, 20	Tensile, flexural	[133–135]
	Glass fibre	ABS	30 (vol%)	Tensile	[136]
		nylon	13.87 (vol%)	Tensile, flexural, impact	[137,138]

### 3. Processing Parameter of FDM

The process parameters influence the material's accuracy, efficiency, and characteristics. As a result, a fundamental study into numerous process factors must be included to produce functionally efficient parts by utilising the FDM technology. Therefore, the FDM printing process specifies and briefly describes several parameters.

#### 3.1. Layer Height

Figure 7 shows the bar chart for layer height used in the FDM process 3D printer. Nearly half of the 100% for layer height is 0.2 mm, consisting of 48%. Most FDM printers only have a size up to a 0.4 mm printing nozzle. The least-used layer height is 0.5 mm. The layer height is also defined as layer thickness. It means the thickness of material extruded from the printing nozzle for printing the physical part. The layer height can be adjusted to the printed parts' referenced thickness. It represents the number of layers formed in a single pass all along the vertical axis of the FDM machine. Material deposition heights will be smaller than the nozzle diameter of the extruder.

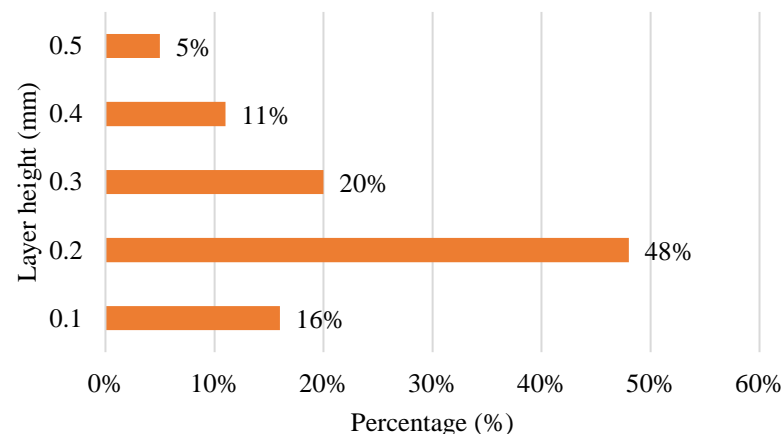


Figure 7. Layer heights used in FDM machine during printing process.

The value is solely dependent on the diameter of the extruder tip. Layer height has an unavoidable impact on the impact and bending properties of the fabricated product. A minimum layer thickness is recommended to obtain better bending properties, and to increase layer thickness as it improves impact properties [139,140]. Compared to other parameters such as shell thickness and part orientation, the impact of layer thickness, as discussed in the literature, contributes roughly 85% of FDM-produced parts' accuracy [141]. Based on the ANOVA results, other studies also show its significance (12.23% contribution)



following the raster width parameter. The part dimension and layer thickness are determined to have a direct correlation. This indicates that thicker layers yield larger pieces, resulting in more significant dimensional variances [142].

### 3.2. Nozzle Temperature

Extrusion temperature is the temperature controlled inside the heating nozzle of FDM even before the material is extruded [143]. It changes the viscosity of printing material, affecting the part's properties. The ideal temperature must be maintained since it can impact the viscosity of the filament material, which affects the printed part. Figure 8 shows the various nozzle temperatures used for the FDM process. The highest temperature used is from 230 °C to 259 °C. The second-highest range is 200 °C to 229 °C. Others stand for ranges from 380 °C to 409 °C, 410 °C to 439 °C, and 440 °C to 469 °C. As the material is extruded from the nozzle, the internal tension develops as the temperature of the material cools from the initial temperature to the temperature of the chamber. This occurs as a result of variations in deposition speed. The internal stress can cause interlayer and intralayer deformation, leading to manufactured part failure [144]. The nozzle temperature melts the filament into a semi-liquid state to print the physical parts. The extrusion temperature would be an essential parameter because if the temperature were low, the material would have a high viscosity which would be hard to extrude. However, if it is too high, the substance will flow, and dripping might occur. As a result, it is vital to fix the extrusion temperature to the correct value, depending on the material used for printing [141].

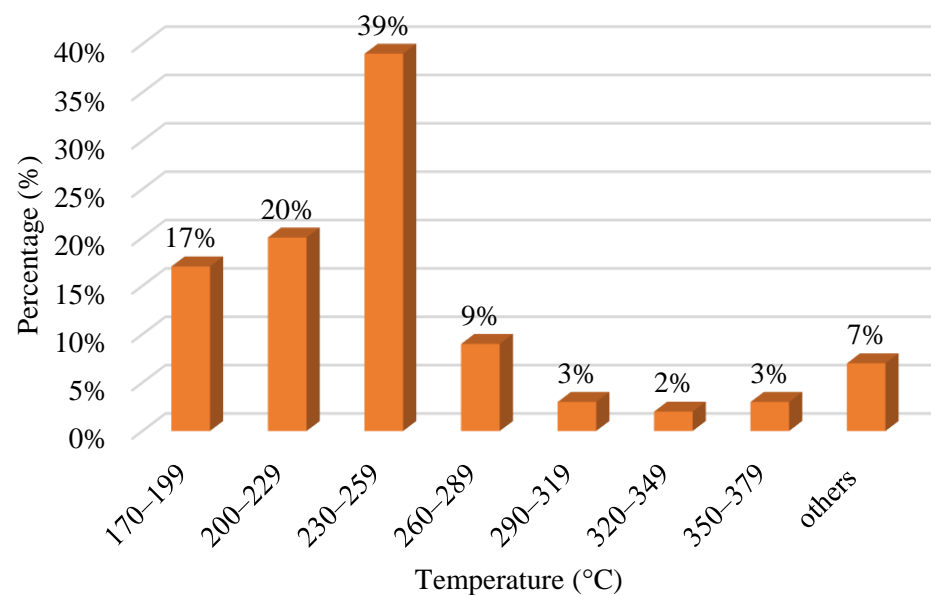


**Figure 8.** Range of nozzle temperature for various material via FDM process.

### 3.3. Bed Temperature

Besides nozzle temperature, bed temperature also plays a vital role in printing. Bed temperature, commonly known as heat bed, is a platform whereby the part is printed during printing. Bed temperature has two primary purposes. Firstly, it can prevent the printing object from warping. Warping is a familiar problem when the edges of the printed material are cooled at various rates compared to the rest of the material. When a heated and stretched material is extruded onto the cold and contracted material, it causes tensions in the material after the new layer cools. This causes the cooled plastic to warp upwards and changes the appearance of the print. Secondly, it helps in layer adhesion. It increases the surface energy of the print bed to improve the bonding strength of the first layer. The prints will not adhere properly to the build plate if the first layer adhesion is poor, which increases the possibility of a print failure. When it has good adhesion, it helps to reduce the

warping of the printing material. Besides preventing warping and layer adhesion, the bed temperature also retains the temperature of the printing platform. The bed temperature also eases the removal process of printed parts. The removal process is straightforward with the bed temperature by using any cutting tools or forces. Figure 9 shows a column chart for the bed temperature of the FDM process. The highest range used is from 50 °C to 70 °C with 39%. The second primarily used range lies from 100 °C to 124 °C, with 18%. The minor range used is 125 °C to 149 °C. Others are ranged from 175 °C to 199 °C and from 200 °C to 224 °C.

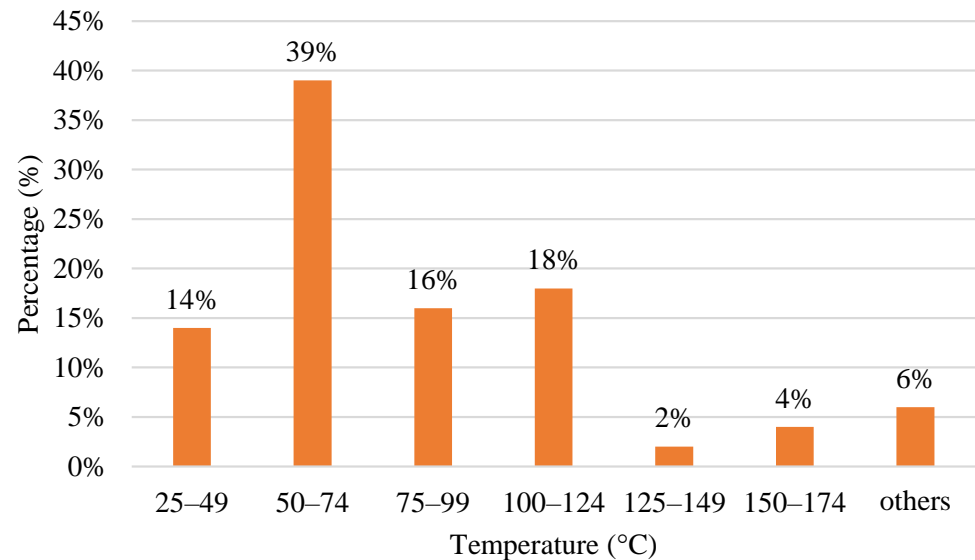


**Figure 9.** The range for bed temperature used in the FDM process for various material.

### 3.4. Printing Speed

In 3D printing technology, print speed is the most critical setting. As the name implies, print speed determines how fast the motors of the printer move. The electric motors controlling the X- and Y-axes and the extruder are included in the printing speed. The speed of the nozzle represents the deposition of filaments over a region of the built component during deposition. Printing speed is equal to the amount of time taken to print. It has a significant influence on the quality of the fabricated model. However, in narrower layer printing, the impact of the printing speed is negligible [145]. Figure 10 shows the printing speed used in the FDM process. The frequently used printing speed is around 21 mm/s to 40 mm/s. The next is 41 mm/s to 60 mm/s.

### 3.5. Building Orientation

Building orientation is also known as building direction. Besides the layer resolution, the build orientation is also very crucial to the process. The building orientation is the angle at which the part is placed about the horizontal axis of the build platform. Surface roughness and staircase effect are determined by resolution, whereas print quality and layer arrangement are determined by build orientation, and fusion is proportional to the mechanical properties of the printed object [14,146]. It describes how parts are positioned on the build platform about the three primary axes of the machine tool, which are the X-axis, Y-axis, and Z-axis [147]. Figure 11 shows the printing orientation of the impact test sample for 0°, 45°, and 90°. Afrose [148] observed that specimens' best strain energy storage capacity and fatigue life are printed at a 45-degree angle.

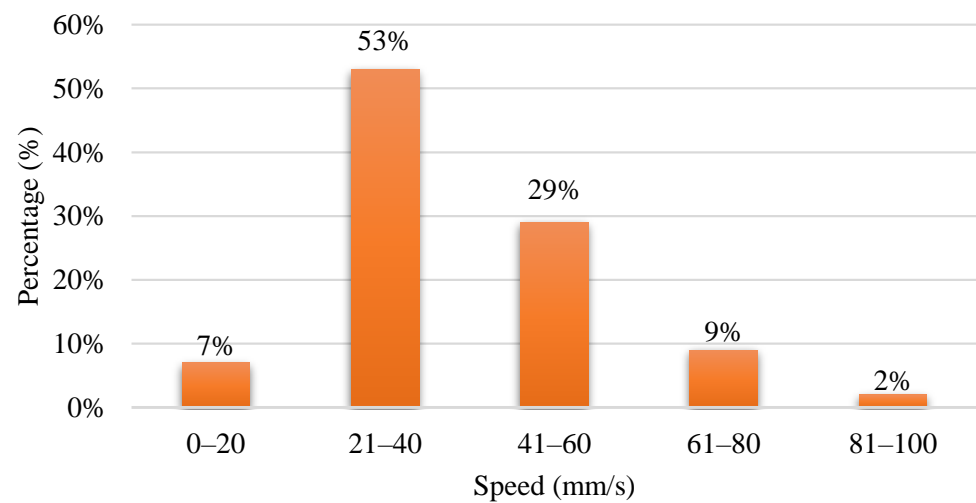


**Figure 10.** Range of printing speed used in FDM process.

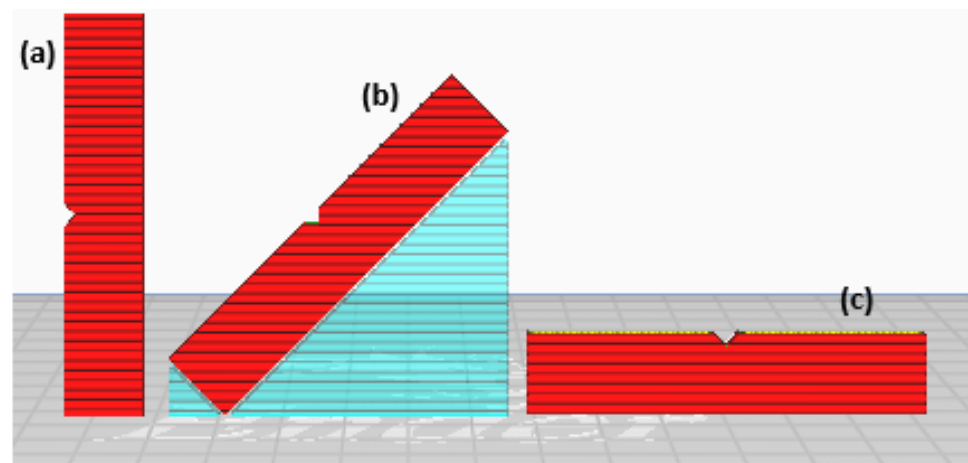


**Figure 11.** Impact samples printed with various (a) 90°, (b) 45°, and (c) 0° building orientations.

### 3.6. Screw Type

#### 3.6.1. Single Screw Extruder

The single screw extruder was invented in the 1870s. It is the most extensively used extruder due to its ease of operation in polymer and rubber production [149]. The most basic single screw extruder configuration is a single revolving screw positioned inside a static cylindrical barrel split into three distinct zones: the compression zone, feed zone, and metering zone [150]. Different pressures can be generated along the length of the screw by varying the depth and pitch of the screw flight within every zone. The screw flight pitch and depth are generally chosen at bigger scales than from other zones to achieve low pressure at the feed zone, which consistently feeds material from the hopper into the extruder barrel [151]. Solid materials must be melted and homogenised as part of the rotating conveyance into the compression zone to form a suitable shape for distribution in the metering zone. As a result, the decreasing screw flight and pitch depth cause a progressive increase in barrel pressure along the length of the compression zone [152]. For less demanding applications, kneading, devolatilising, and mixing can be conducted in this processing zone [152,153]. A homogenous product by consistent structure can be achieved from die extrusion by stabilising the effervescent flow to a steady condition in the last metering zone. Fabricating extrusion-based goods using a single screw extruder is particularly well suited for high viscosity polymers since it may produce high pressure during operation [154].

The material is fed into the barrel through the feed throat by gravity force, and in most single screw extruders, the speed of the screw controls the output rate. High pressure to transfer material from the feed system causes the plastic pellet or powder to condense into a solid bed [155]. Periodically, the mass flow rate is unaffected by the speed of the screw and is regulated directly from the feed system by using a starving fed mechanism, resulting in an output rate that is lower than the forwarding efficiency of the screw [156,157]. The single screw extruder has only one screw and is used to make homogeneous polymers in a continuous shape [149,158]. Single screw extruders are unsuitable for heat-sensitive polymers due to higher friction and thermal energy as the screw speed increases.

Furthermore, significant pressure is used during the extrusion process, compressing the ingredients to generate filaments. However, it may lead to agglomeration and poor mixing due to a lack of shear deformation. [159–161].

### 3.6.2. Twin Screw Extruder

Although the single screw extruder process seems simple and inexpensive, it lacks the mixing capacity required to produce a polymer composite using many compounded components. As a result, in the late 1930s, a modified extruder known as a twin screw extruder that contained two screws placed next to each other at a modular barrel was developed to form intimate blends of two or more different materials [162]. Unlike a single screw extruder, a twin screw extruder provides a more vital shear force amongst the screws and barrel and the rotating screws, resulting in the proper mixing of materials [163]. As a result, a broad range of mixing operations and heat transfers are achieved with a faster throughput, independent of the screw's speed. On the other hand, the counter-rotating system can generate a sizeable extensional shear force between the gaps between the two screws, allowing for a significant potential air entrapment, pressure generation, and extended retention period while using the minimal speed and output of the screw [164,165]. Both can be divided into two categories: entirely intermeshing and non-intermeshing. Because of its self-wiping function, the intermeshing twin screw extruder may not only eliminate non-motion throughout the extrusion, but also avoid excessive overheating of raw materials. After the process, the rotation of the screws removes residual material from the screw roots and cleans the entire inside barrel. Table 3 shows the difference of single screw extruder and twin screw extruder.

Meanwhile, this popular layout can help reduce product waste at the end of the manufacturing process [166]. The mutually different screws positioned in the extruder barrel for the non-intermeshing type result in low torque generation and weak interaction, making it a better choice for processing high viscosity materials and venting to eliminate interior volatile substances [167]. Figure 12 shows the type of screws.

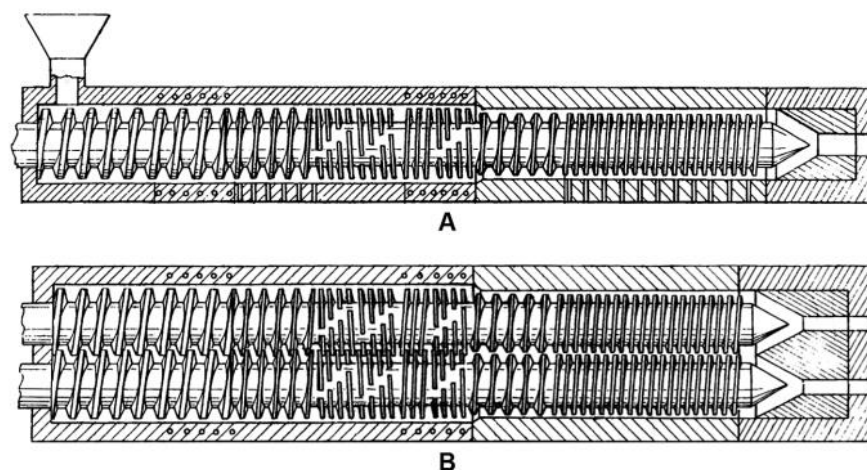


**Figure 12.** (A) single screw extruder and (B) twin screw extruder. Adapted with permission from Uitterhaegen [168]. 2017, Elsevier.

**Table 3.** Single screw and twin screw are compared.

Extrusion Type (Screw)	Extruder Model	Advantages	Disadvantages	Reference
Single	SJ-30/25, Zhangjiagang Grand	Cheap Simple design Low maintaining cost	Poor in mixing Not suitable for low heat-resistant materials	[169–172]
Twin	SJ-30/25, Zhangjiagang Grand APV Chemical Machinery MP 2015 DSM Xplore Haake Rheomex OS, Thermo Fisher, Germany	High dispersion capacity, which results in better mixing Better process parameters control Easy material feed Flexible and better productivity	Expensive Better input energy Not applicable for materials that are shear-sensitive	[171–175]

#### 4. Properties of FDM-Polymer Composite

##### 4.1. Mechanical Analysis

Mechanical properties are testing aids in evaluating and designing materials and products, allowing them to last longer and be more efficient and cheaper. AM polymers' characteristics are tested using ASTM and ISO test methods. They also aid in the creation of desired items. In order to prepare the sample and conduct mechanical experiments, research organisations use ASTM standard criteria; for example, practically all research groups evaluated for tensile tests [176,177] employ ASTM D638. The majority of research findings state that the component's ultimate tensile strength, yield strength, elasticity, and elongation are mostly affected by the process parameters. Figure 13 shows the mechanical properties that were tested from 2011 to 2021. From the study conducted, the most tested mechanical property is tensile. Flexural is the second most thoroughly tested mechanical property. Fatigue behaviour is one of the mechanical properties that has undergone minor testing. The tensile test is used on samples to determine material parameters, such as ultimate tensile strength, yield stress, Young's modulus, ductility, and toughness. There are many shapes and designs to choose from when producing a sample for the tensile test. Even though there are various options for the test sample design, it must adhere to ASTM standards [178].

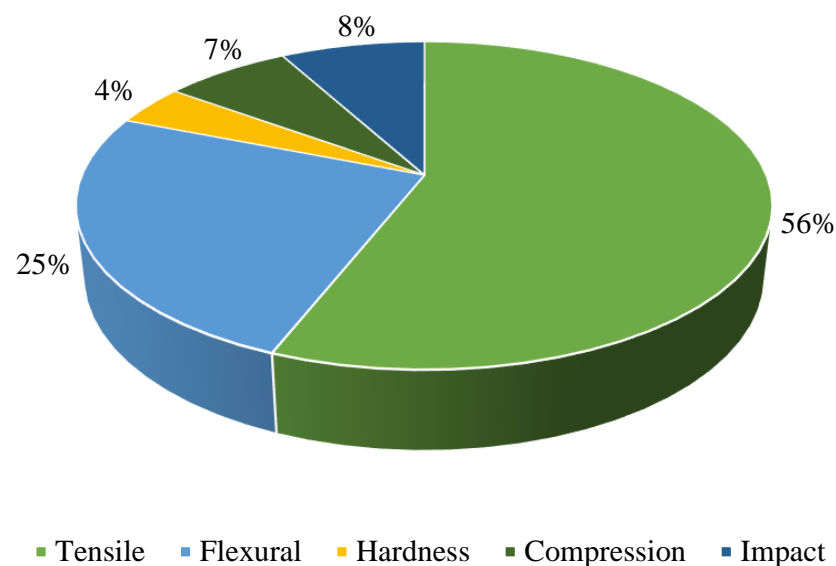


**Figure 13.** Mechanical properties that were studied primarily in the FDM process from the year 2011 to 2021.

The advancement of the fibre composite by using the FDM technique has expanded opportunities for field research. The tensile properties of composites are heavily influenced by factors such as printing parameters, fibre content, and fibre reinforcement. The percentage of fibre reinforcement and the orientation of fibres determine the tensile strength of the composite produced by the FDM process [179,180]. The interlaminar shear strength of the FDM-fabricated fibre composite is compromised, which directly impacts the flexural strength of composites. In addition, the FDM-fabricated fibre composite has anisotropic properties that cause variations in strain rate when bending, which increase the shear stress amongst the layers, and ultimately cause the separation of layers and failure. Therefore, the interlaminar shear strength is an essential factor to consider when improving the flexural properties of the FDM-printed fibre composites [181]. In order to significantly increase the mechanical qualities of FDM 3D-printed PLA items, such as average tensile strength and impact toughness, Kuan et al. [182] and Li et al. [183] created FDM printing filaments containing carbon fibre and MWCNT for the reinforced phase-modified PLA.

#### 4.2. Thermal Analysis

Figure 14 shows a chart of thermal analyses. There are three types of thermal analyses: dynamic mechanical analysis (DMA), thermogravimetric analysis (TGA), and differential scanning calorimetry (DSC). The highest thermal analysis used is DSC with 41%, while TGA is 31%. Essential qualities of energetic materials are their thermal properties, which are strongly related to safety during manufacturing, storage, transportation, and usage. The thermal properties of energetic materials can be determined quickly, efficiently, and effectively using thermal analysis tools [184]. However, in thermal analysis investigations, the fluctuation of thermogravimetry (TGA) curves frequently occurs for unknown reasons, and the mass-loss curves, for example, grow or drop drastically and even surpass the complete scales of instruments. Furthermore, the differential scanning calorimetry/differential thermal analysis (DSC/DTA) is inconsistent with TG because the crucible frequently shifts or slips off the sample pan [185]. Table 4 shows the difference between TGA and DSC.

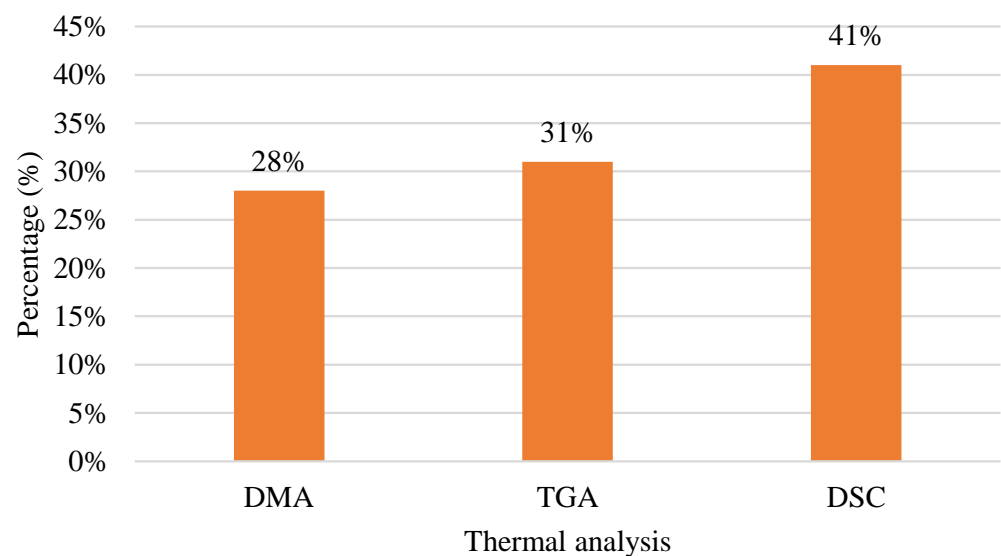


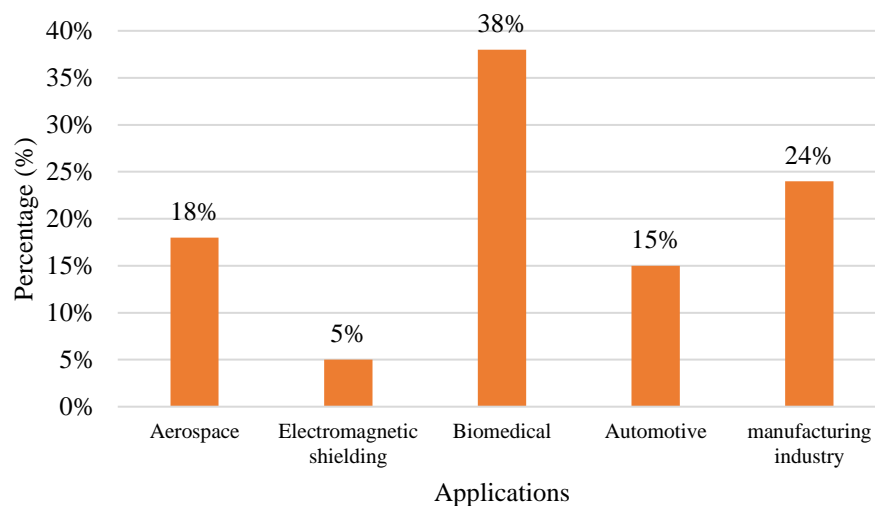
**Figure 14.** Thermal analysis of FDM polymer composite from the year 2011 to 2021.

**Table 4.** Comparison of TGA and DSC.

	TGA	DSC	Reference
Primary determination	Changes in sample mass as a function of temperature or time	Changes in heat flow to and from a sample as a function of temperature or time	[92,186,187]
Temperature range	Room temperature to 1000 °C	−170 °C to 600 °C	[188–190]
Sample amount	Approximately 5–50 mg	Approximately 5–50 mg	[191–193]
Typical output	Lost or gained % by mass Residual mass	Transition temperature Transition enthalpy	[194,195]
Example of applications	Moisture content Decomposition Thermal stability Compositional analysis Oxidation	Phase transitions: melting and crystallisation Glass transition Solid–solid transitions	[196–198]

## 5. Application of Polymer Composite in 3D Printing

Various industries are using the FDM process to produce products. Figure 15 shows the FDM application in industries. The biomedical field is one industry that utilises the FDM process for its product, whereby the industry utilises 38% out of 100%. Manufacturing is the second-highest industry in utilising the FDM process, and aerospace is the third-highest industry. In recent times, the use of FDM technology has grown in popularity, particularly in aerospace, medical, and automobile fields. In addition, the overall quality of prototypes printed for the aerospace sector is in high demand since they are utilised to examine the fluid dynamic behaviour of models [141].

**Figure 15.** Application of FDM using polymer composite.

### 5.1. Aerospace

In the past few years, the production of aircraft, satellites, and space shuttles has drastically increased the demand for aerospace and aviation components [199]. Aerospace components with a high aesthetic value rather than high efficiencies, such as light housings, door handles, power wheels, and complete dashboard designs, are usually made using 3D printing. Metal 3D printing enables the manufacture and deployment of complex military components more quickly [200]. However, recycling scrap formation after manufacturing aircraft parts is costly and time-consuming. As much as 80–90% of the conventional billet may be wasted during machining, but an AM process can reduce this by less than 10%. AM also allows the creation of free-form designs that produce tooling fixtures for making expensive aerospace materials such as titanium. As a result, conventional manufacturing



methods can only produce cooling channels with straight lines, complicating aerospace components' fluid flow optimisation [201]. Figure 16 shows Stratasy's and Aurora Flight Sciences' AM-unmanned aerial vehicle (UAV).



**Figure 16.** UAV using the FDM process. Adapted with permission from Stratasy's [202].

### 5.2. Automotive

An AM technique widely used is fused deposition modelling (FDM). It is used in the automobile industry for various purposes, including lightweight equipment, final functional components, and testing models. On the other hand, the FDM technology faces two significant challenges in becoming a viable processing method in the automotive industry, which are weak and anisotropic mechanical characteristics and a limited range of printing materials. The mechanical properties of FDM's physical parts are influenced by weak interlayer links produced during the layer top layering process [203]. By design, the brake pedal is one of the most critical pieces of the vehicle. A brake pedal is a safety component with sound engineering, exact quality requirements, and critical quality inspection. In addition, the brake pedal is the most acceptable option for research because of its severe characteristics. As a result, if a crucial part can be produced with the AM technique, then less critical parts such as brackets, hinges, and supports, to name a few, can also be produced [9]. Figure 17 shows the brake pedal produced by using the FDM process.

### 5.3. Biomedical

Biomedical implants benefit the medical profession and end-users, such as people who have suffered severe accidents or illnesses. However, biomedical implants are artificial substitutes expected to function similarly to the original. Therefore, any substance used as an implant must be compatible with the human body [204]. Because of its ability to provide personalised fabrication at a minimal cost, 3D technology has piqued the interest of industrial and academic fields. In addition, 3D printing technology enables the creation of polymeric materials for biomedical applications due to inherent advantages, such as the capacity to create complicated geometry quickly. There are four broad study categories in which the latest 3D printing technology developed for medical application can be classified as the formation of diseased organs, development of permanent non-bioactive implants, and development of biodegradable and bioactive scaffolds on organ and tissue printing [205]. In addition, the FDM-fabricated bone prototypes can be used in biomedical research and real-world testing; these can be 3D solid models, specimens for similar

mechanical prototypes, and mechanical testing. Geometric parameters, as well as local or global mechanical properties, can be evaluated by the models showed in Figure 18 [206].



**Figure 17.** Metal brake pedal using BASF Ultra fuse 316L metal-polymer filament via FDM. Adapted with permission from Sargini et al. [9]. 2021, Elsevier.

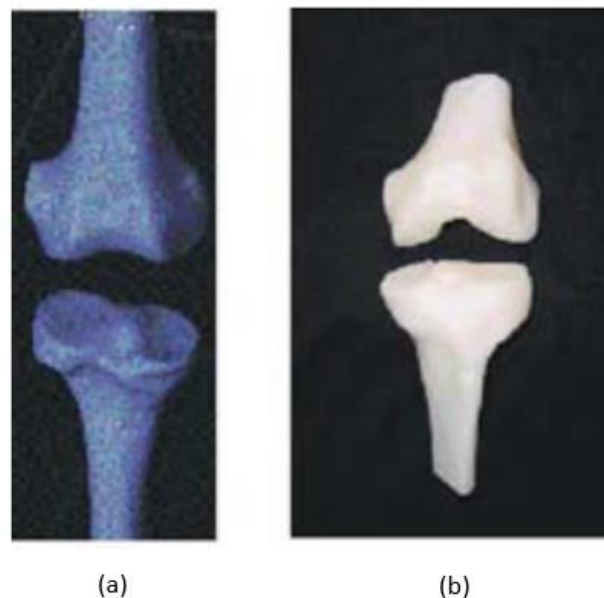


**Figure 18.** (a) Geometric model and (b) FDM prototype of femur and tibia. Adapted with permission from Revilla-León et al. [206]. 2002, IOP Conference Science.

#### 5.4. Textile

Textile companies are also beginning 3D printing to fabricate dresses, shoes, and other items [207]. Good adhesion and stability are the primary factors in textile manufacturing [208]. Polylactic acid (PLA), acrylonitrile butadiene styrene (ABS), polyamide (PA), and polycarbonate (PC) are usually used in FDM. In addition, fibres, fillers, dyes, and other additives are commonly used to produce filaments [209,210]. The widespread application of PLA and Soft PLA is used to print smooth, glossy, soft, and lacelike fabric structures, because they are more flexible than PA and ABS and give the end product a soft handle [207]. On the flip side, ABS is rigid, making it suitable for joints [210,211]. According

to Samit et al. researchers have constructed various knitted structures and weaves using the FDM process, such as woven fabric structures with weft knitted structures and visible stitches. They have also experienced using FDM printing to create garment panels, lace structures, and composite structures [207,209,211,212]. Figure 19 shows an FDM-printed structure for textile.

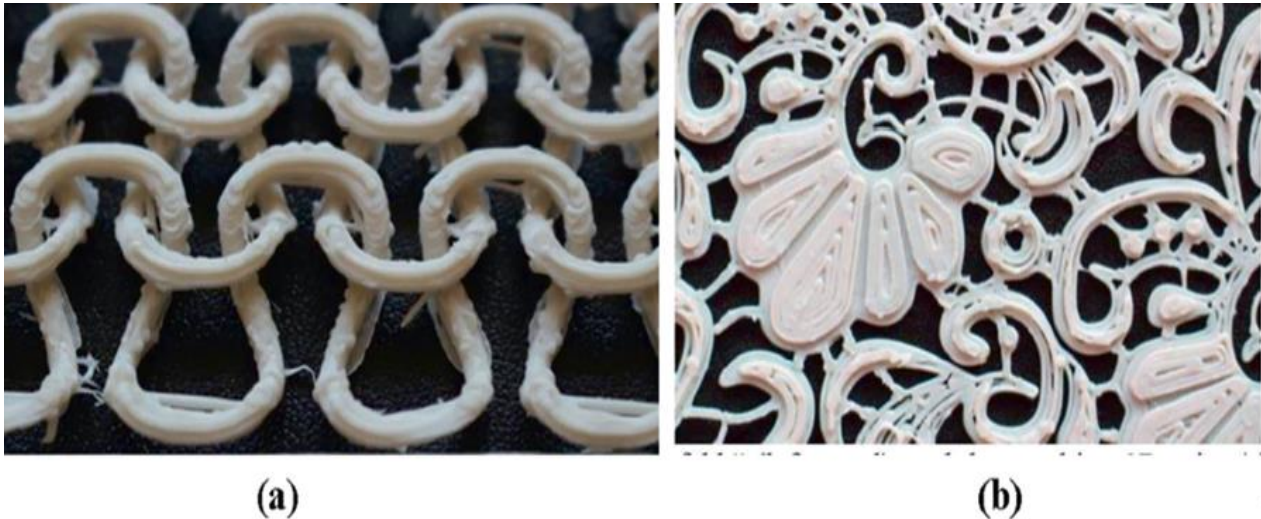


**Figure 19.** (a) 3D-printed weft knit and (b) lace structure in textile industry. Adapted with permission from Chakraborty et al. [212]. 2020, Elsevier.

### 5.5. Functional Materials

Functional materials are typically defined as those that have specific inherent qualities and functions of their own. Topology optimisation is a popular and effective method for determining structural configurations for various performance types. Additionally, it is viable to incorporate it into additive manufacturing. Chen et al. have built topological structures with an effective zero Poisson's ratio: a framework based on periodic unit cells with plus-minus Poisson's ratios established. The topologically designed structures are then printed using 3D printing technology and short carbon fibre reinforced polyamide (SCF/PA) [213]. The auxetic effect, also known as the negative Poisson ratio (NPR), can be induced in a hexagonal honeycomb by changing the cell angles. To achieve better mechanical properties and functionality, continuous carbon fibre (CCF)-reinforced composites are designed and 3D-printed by Chen et al. [214]. Furthermore, for the planar lattice designs, a center cross-lattice with four outer-strip components is created using carbon fibre-reinforced polyamide composites via FDM by Chen et al. [215]. Auxetic geometries are then turned into high-performance composites via the 3D printing technique, reinforced with chopped carbon fibre (CF). The effects of polynomial ordering and CF incorporation on the mechanical properties are carefully investigated by Hu et al. [216]. Chen et al. have studied the compressive behaviours of 3D-printed CF-reinforced polyamide composite metamaterials with NPR [217].

## 6. Future Trend/Challenges of FDM-Polymer Composite

Figure 20 shows the trend of polymer composite utilisation in the FDM process from 2011 to 2021. The graph shows that the trend is increasing yearly. From the study conducted, the utilisation of polymer composite had a drastic hike in 2017 and 2021 compared to the other years.

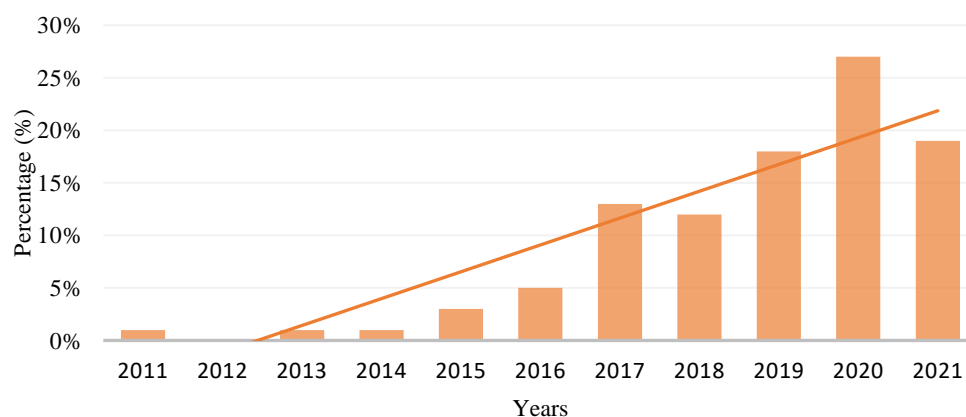


**Figure 20.** The trend of polymer composition utilisation in FDM from year 2011 to 2021.

The use of AM and other advanced manufacturing technologies such as the FDM process is ushering in a new era in manufacturing, whereby value chains are short, tiny, more localised and personalised, cooperative, and sustainable. Compared to the typical subtractive techniques, these are potentials that enhance resource efficiency, reduce waste of expensive metals such as titanium, and enhance the design for assembly methods to improve characteristics and lower costs.

There are many signs to suggest that the FDM process will continue to be integrated into current industrial processes and human life as the technology develops and becomes more affordable. As a result, the FDM sector, comprising technology and material advancements, as well as related services, has grown at an exponential rate.

## 7. Conclusions

AM is one of the most significant accomplishments of the fourth industrial revolution. The uses of AM have significant growth in many industries. FDM is the most popular AM due to its endless benefits. FDM is a process that can produce various complex designs into physical objects at a lower cost as compared to traditional manufacturing. This article discusses:

1. An overview of FDM process flow and polymer composite material properties, and the type of base and filler material commonly used in FDM.
2. The printing parameters such as nozzle temperature, bed temperature, printing speed, building orientation, layer height, and screw type also play a significant role in the performance of the FDM-printed product. However, the relationship between printing quality and mechanical behaviour for the various types of materials used in FDM cannot be explained by the available data. There are currently no absolute laws and regulations that can be applied to help users improve the printing process to achieve the best printing results, because the same printing procedure can result in various printing outcomes if the material is different.
3. Different polymers have different behaviours in terms of mechanical properties. Adding fillers to thermoplastic polymers can enhance the properties and strength of that particular polymer. Meanwhile, it is still rare to come across the improvement of process parameters for thermal, chemical, and dynamic mechanical properties.
4. The application of the FDM process in industries such as the aerospace, automobile, textile, and biomedical sectors is also explained briefly. However, in terms of large-scale applications, FDM still cannot be used as a substitute for the traditional technique, such as injection moulding, when analyzing the mechanical work performance achieved. The main issues with the FDM printing are porosity, gaps between layers, and rasters produced in the FDM process.



**Author Contributions:** Conceptualization, J.M. and W.S.W.H.; resources, K.K.; data curation, D.R.; writing—original draft preparation, J.M.; writing—review and editing, J.M. visualization, A.B.S.; supervision, W.S.W.H.; project administration, F.T. and F.A.; funding acquisition, F.M.F. and W.S.W.H. All authors have read and agreed to the published version of the manuscript.

**Funding:** The research was funded by Universiti Malaysia Pahang, grant numbers RDU 1901135, PGRS210367, PGRS210377, and FRGS/1/2019/TK03/UMP/02/15.

**Institutional Review Board Statement:** Not applicable.

**Data Availability Statement:** Not applicable.

**Acknowledgments:** The authors thank the Universiti Malaysia Pahang for the Research Grants RDU 1901135, PGRS210367, PGRS210377, and Fundamental Research Grant Scheme under FRGS/1/2019/TK03/UMP/02/15 for their financial assistance and laboratory facilities during the project.

**Conflicts of Interest:** The authors declare no conflict of interest.

## References

1. Hart, K.R.; Wetzel, E.D. Fracture behavior of additively manufactured acrylonitrile butadiene styrene (ABS) materials. *Eng. Fract. Mech.* **2017**, *177*, 1–13. [[CrossRef](#)]
2. Almuallim, B.; Harun, W.S.W.; Rikabi, I.J.R.; Mohammed, H.A. Thermally conductive polymer nanocomposites for filament-based additive manufacturing. *J. Mater. Sci.* **2022**, *57*, 3993–4019. [[CrossRef](#)]
3. Patil, P.; Singh, D.; Raykar, S.J.; Bhamu, J. Multi-objective optimization of process parameters of Fused Deposition Modeling (FDM) for printing Polylactic Acid (PLA) polymer components. *Mater. Today Proc.* **2021**, *45*, 4880–4885. [[CrossRef](#)]
4. Harun, W.S.W.; Kamariah, M.S.I.N.; Muhamad, N.; Ghani, S.A.C.; Ahmad, F.; Mohamed, Z. A review of powder additive manufacturing processes for metallic biomaterials. *Powder Technol.* **2018**, *327*, 128–151. [[CrossRef](#)]
5. Kumar, R.; Kumar, M.; Chohan, J.S. The role of additive manufacturing for biomedical applications: A critical review. *J. Manuf. Processes* **2021**, *64*, 828–850. [[CrossRef](#)]
6. Talib, S.; Gupta, S.; Chaudhary, V.; Gupta, P.; Wahid, M.A. Additive manufacturing: Materials, techniques and biomedical applications. *Mater. Today Proc.* **2021**, *46*, 6847–6851. [[CrossRef](#)]
7. Blakey-Milner, B.; Gradl, P.; Snedden, G.; Brooks, M.; Pitot, J.; Lopez, E.; Leary, M.; Berto, F.; Plessis, A. Metal additive manufacturing in aerospace: A review. *Mater. Des.* **2021**, *209*, 110008. [[CrossRef](#)]
8. Najmon, J.C.; Raesi, S.; Tovar, A. Review of additive manufacturing technologies and applications in the aerospace industry. In *Additive Manufacturing for the Aerospace Industry*; Froes, F., Boyer, R., Eds.; Elsevier: Amsterdam, The Netherlands, 2019; pp. 7–31.
9. Sargini, M.I.M.; Masood, S.H.; Palanisamy, S.; Jayamani, E.; Kapoor, A. Additive manufacturing of an automotive brake pedal by metal fused deposition modelling. *Mater. Today Proc.* **2021**, *45*, 4601–4605. [[CrossRef](#)]
10. Jimeno-Morenilla, A.; Azariadis, P.; Molina-Carmona, R.; Kyratzi, S.; Moulitanitis, V. Technology enablers for the implementation of Industry 4.0 to traditional manufacturing sectors: A review. *Comput. Ind.* **2021**, *125*, 103390. [[CrossRef](#)]
11. Jayaraghu, T.K.; Karthik, K.; Yaswanth, A.; Venkatesan, M. Nozzle flow characteristics of P.E.E.K (Poly-ether ether ketone) material used in 3D-printing. *Mater. Today Proc.* **2021**, *44*, 2963–2967. [[CrossRef](#)]
12. Deomore, S.A.; Raykar, S.J. Multi-criteria decision making paradigm for selection of best printing parameters of fused deposition modeling. *Mater. Today Proc.* **2021**, *44*, 2562–2565. [[CrossRef](#)]
13. Stoia, D.I.; Marsavina, L. Effect of Aluminum Particles on the Fracture Toughness of Polyamide-based Parts Obtained by Selective Laser Sintering (SLS). *Procedia Struct. Integr.* **2019**, *18*, 163–169. [[CrossRef](#)]
14. Khan, S.; Joshi, K.; Deshmukh, S. A comprehensive review on effect of printing parameters on mechanical properties of FDM printed parts. *Mater. Today Proc.* **2021**, *50*, 2119–2127. [[CrossRef](#)]
15. Ahmed, N. Direct metal fabrication in rapid prototyping: A review. *J. Manuf. Process.* **2019**, *42*, 167–191. [[CrossRef](#)]
16. Ahn, D.; Kweon, J.; Choi, J.; Lee, S. Quantification of surface roughness of parts processed by laminated object manufacturing. *J. Mater. Process. Technol.* **2012**, *212*, 339–346. [[CrossRef](#)]
17. Derby, B. Additive Manufacture of Ceramics Components by Inkjet Printing. *Engineering* **2015**, *1*, 113–123. [[CrossRef](#)]
18. Revilla-León, M.; Methani, M.M.; Morton, D.; Zandinejad, A. Internal and marginal discrepancies associated with stereolithography (SLA) additively manufactured zirconia crowns. *J. Prosthet. Dent.* **2020**, *124*, 730–737. [[CrossRef](#)]
19. Giri, J.; Shahane, P.; Jachak, S.; Chadge, R.; Giri, P. Optimization of FDM process parameters for dual extruder 3d printer using Artificial Neural network. *Mater. Today Proc.* **2021**, *43*, 3242–3249. [[CrossRef](#)]
20. Angelopoulos, P.M.; Samouhos, M.; Taxiarchou, M. Functional fillers in composite filaments for fused filament fabrication; a review. *Mater. Today Proc.* **2021**, *37*, 4031–4043. [[CrossRef](#)]
21. Dehghan-Manshadi, A.; Yu, P.; Dargusch, M.; StJohn, D.; Qian, M. Metal injection moulding of surgical tools, biomaterials and medical devices: A review. *Powder Technol.* **2020**, *364*, 189–204. [[CrossRef](#)]
22. Maurya, R.K.; Niranjana, M.S. An experimental analysis of process parameters for EN-36C alloy steel using CNC lathe—A review. *Mater. Today Proc.* **2020**, *25*, 773–777. [[CrossRef](#)]

23. Doungkom, P.; Jiamjiroch, K. Analysis of Printing Pattern and Infiltration Percent over the Tensile Properties of PLA Printed Parts by a Fuse Deposition Modelling Printer. *IOP Conf. Ser. Mater. Sci. Eng.* **2019**, *501*, 012028. [[CrossRef](#)]
24. Wickramasinghe, S.; Do, T.; Tran, P. FDM-based 3D printing of polymer and associated composite: A review on mechanical properties, defects and treatments. *Polymers* **2020**, *12*, 1529. [[CrossRef](#)]
25. Thomas, S.; Joseph, K.; Malhotra, S.K.; Goda, K.; Sreekala, M.S. Polymer composites. In *Macro- and Microcomposites*; John Wiley & Sons: Hoboken, NJ, USA, 2012; Volume 1.
26. Asim, M.; Saba, N.; Jawaaid, M.; Nasir, M. Potential of natural fiber/biomass filler-reinforced polymer composites in aerospace applications. In *Sustainable Composites for Aerospace Applications*; Jawaaid, M., Thariq, M., Eds.; Woodhead Publishing: Sawston, UK, 2018; pp. 253–268.
27. Gavali, V.C.; Kubade, P.R.; Kulkarni, H.B. Property Enhancement of Carbon Fiber Reinforced Polymer Composites Prepared by Fused Deposition Modeling. *Mater. Today Proc.* **2020**, *23*, 221–229. [[CrossRef](#)]
28. Shanmugam, V.; Rajendran, D.J.J.; Babu, K.; Rajendran, S.; Veerasimman, A.; Marimuthu, U.; Singh, S.; Das, O.; Neisiany, R.E.; Hedenqvist, M.S.; et al. The mechanical testing and performance analysis of polymer-fibre composites prepared through the additive manufacturing. *Polym. Test.* **2021**, *93*, 106925. [[CrossRef](#)]
29. Vyavahare, S.; Teraiya, S.; Panghal, D.; Kumar, S. Fused deposition modelling: A review. *Rapid Prototyp. J.* **2020**, *26*, 176–201. [[CrossRef](#)]
30. Singh, A.P.; Sharma, M.; Singh, I. A review of modeling and control during drilling of fiber reinforced plastic composites. *Compos. Part B Eng.* **2013**, *47*, 118–125. [[CrossRef](#)]
31. Dandekar, C.R.; Shin, Y.C. Modeling of machining of composite materials: A review. *Int. J. Mach. Tools Manuf.* **2012**, *57*, 102–121. [[CrossRef](#)]
32. Koli, D.K.; Agnihotri, G.; Purohit, R. Properties and characterization of Al-Al<sub>2</sub>O<sub>3</sub> composites processed by casting and powder metallurgy routes. *Int. J. Latest Trends Eng. Technol. (IJLTET)* **2013**, *2*, 486–496.
33. Clyne, T.W.; Hull, D. *An Introduction to Composite Materials*, 3rd ed.; Cambridge University Press: Cambridge, UK, 2019.
34. Gibson, R.F. A review of recent research on mechanics of multifunctional composite materials and structures. *Compos. Struct.* **2010**, *92*, 2793–2810. [[CrossRef](#)]
35. Mittal, V.; Saini, R.; Sinha, S. Natural fiber-mediated epoxy composites—A review. *Compos. Part B Eng.* **2016**, *99*, 425–435. [[CrossRef](#)]
36. Qin, Q.; Ye, J. *Toughening Mechanisms in Composite Materials*; Elsevier: Amsterdam, The Netherlands, 2015.
37. Cen, H.; Kang, Y.; Lei, Z.; Qin, Q.; Qiu, W. Micromechanics analysis of Kevlar-29 aramid fiber and epoxy resin microdroplet composite by Micro-Raman spectroscopy. *Compos. Struct.* **2006**, *75*, 532–538. [[CrossRef](#)]
38. Qin, Q.H. Introduction to the composite and its toughening mechanisms. In *Toughening Mechanisms in Composite Materials*; Woodhead Publishing Series in Composites Science and Engineering; Woodhead Publishing: Sawston, UK, 2015; pp. 1–32.
39. Tsai, S.W.; Hahn, H.T. *Introduction to Composite Materials*; Routledge: Boca Raton, FL, USA, 2018.
40. Barbero, E.J. *Introduction to Composite Materials Design*; CRC press: Boca Raton, FL, USA, 2010.
41. Ray, B. Temperature effect during humid ageing on interfaces of glass and carbon fibers reinforced epoxy composites. *J. Colloid Interface Sci.* **2006**, *298*, 111–117. [[CrossRef](#)]
42. Xu, Y.; Chung, D.; Mroz, C. Thermally conducting aluminum nitride polymer-matrix composites. *Compos. Part A Appl. Sci. Manuf.* **2001**, *32*, 1749–1757. [[CrossRef](#)]
43. Davim, J.P.; Reis, P. Study of delamination in drilling carbon fiber reinforced plastics (CFRP) using design experiments. *Compos. Struct.* **2003**, *59*, 481–487. [[CrossRef](#)]
44. Mukherjee, M.; Das, C.; Kharitonov, A. Fluorinated and oxyfluorinated short Kevlar fiber-reinforced ethylene propylene polymer. *Polym. Compos.* **2006**, *27*, 205–212. [[CrossRef](#)]
45. Dang, Z.-M.; Yuan, J.-K.; Zha, J.-W.; Zhou, T.; Li, S.T.; Hu, G.-H. Fundamentals, processes and applications of high-permittivity polymer-matrix composites. *Prog. Mater. Sci.* **2012**, *57*, 660–723. [[CrossRef](#)]
46. Thoppul, S.D.; Finegan, J.; Gibson, R.F. Mechanics of mechanically fastened joints in polymer-matrix composite structures—a review. *Compos. Sci. Technol.* **2009**, *69*, 301–329. [[CrossRef](#)]
47. Wisnom, M.R.; Gigliotti, M.; Ersoy, N.; Campbell, M.; Potter, K.D. Mechanisms generating residual stresses and distortion during manufacture of polymer-matrix composite structures. *Compos. Part A Appl. Sci. Manuf.* **2006**, *37*, 522–529. [[CrossRef](#)]
48. Barekar, N.; Tzamtzis, S.; Dhindaw, B.K.; Patel, J.; Babu, N.H.; Fan, Z. Processing of aluminum-graphite particulate metal matrix composites by advanced shear technology. *J. Mater. Eng. Perform.* **2009**, *18*, 1230–1240. [[CrossRef](#)]
49. Kök, M. Abrasive wear of Al<sub>2</sub>O<sub>3</sub> particle reinforced 2024 aluminium alloy composites fabricated by vortex method. *Compos. Part A Appl. Sci. Manuf.* **2006**, *37*, 457–464. [[CrossRef](#)]
50. Dixit, N.; Jain, P.K. 3D printed carbon fiber reinforced thermoplastic composites: A review. *Mater. Today Proc.* **2021**, *43*, 678–681. [[CrossRef](#)]
51. Park, S.; Fu, K. Polymer-based filament feedstock for additive manufacturing. *Compos. Sci. Technol.* **2021**, *213*, 108876. [[CrossRef](#)]
52. Lay, M.; Thajudin, N.L.N.; Hamid, Z.A.A.H.; Rusli, A.; Abdullah, M.K.; Shuib, R.K. Comparison of physical and mechanical properties of PLA, ABS and nylon 6 fabricated using fused deposition modeling and injection molding. *Compos. Part B Eng.* **2019**, *176*, 107341. [[CrossRef](#)]

53. Penumakala, P.K.; Santo, J.; Thomas, A. A critical review on the fused deposition modeling of thermoplastic polymer composites. *Compos. Part B Eng.* **2020**, *201*, 108336. [[CrossRef](#)]
54. Vlasceanu, D.; Baciuc, F.; Popescu, D.; Hadar, H.; Marinescu, R. Development and 3D Printing of an ABS Ergonomic Handle for Medical Use. *Mater. Plast.* **2018**, *55*, 630. [[CrossRef](#)]
55. Alhallak, L.M.; Tirkes, S.; Tayfun, U. Mechanical, thermal, melt-flow and morphological characterizations of bentonite-filled ABS copolymer. *Rapid Prototyp. J.* **2020**, *26*, 1305–1312. [[CrossRef](#)]
56. Li, X.; Sun, L.; Aifantis, K.E.; Fan, Y.; Feng, Q.; Cui, F.; Watari, F. 3D-printed biopolymers for tissue engineering application. *Int. J. Polym. Sci.* **2014**, *2014*, 829145. [[CrossRef](#)]
57. Fornells, E.; Murray, E.; Waheed, S.; Morrin, A.; Diamond, D.; Paull, B.; Breadmore, M. Integrated 3D printed heaters for microfluidic applications: Ammonium analysis within environmental water. *Anal. Chim. Acta* **2020**, *1098*, 94–101. [[CrossRef](#)]
58. Raney, K.; Lani, E.; Kalla, D.K. Experimental characterization of the tensile strength of ABS parts manufactured by fused deposition modeling process. *Mater. Today Proc.* **2017**, *4*, 7956–7961. [[CrossRef](#)]
59. Kamran, M.; Saxena, A. A comprehensive study on 3D printing technology. *MIT Int. J. Mech. Eng.* **2016**, *6*, 63–69.
60. Zhang, D.; Chi, B.H.; Li, B.W.; Gao, Z.W.; Du, Y.; Guo, J.B.; Wei, J. Fabrication of highly conductive graphene flexible circuits by 3D printing. *Synth. Met.* **2016**, *217*, 79–86. [[CrossRef](#)]
61. Tak, J.; Kang, D.G.; Choi, J. A lightweight waveguide horn antenna made via 3D printing and conductive spray coating. *Microw. Opt. Technol. Lett.* **2017**, *59*, 727–729. [[CrossRef](#)]
62. Narayanan, L.K.; Huebner, P.; Fisher, M.B.; Spang, J.T.; Starly, B.; Shirwaiker, R.A. 3D-bioprinting of polylactic acid (PLA) nanofiber–alginate hydrogel bioink containing human adipose-derived stem cells. *ACS Biomater. Sci. Eng.* **2016**, *2*, 1732–1742. [[CrossRef](#)]
63. Levato, R.; Visser, J.; Planell, J.A.; Engel, E.; Malda, J.; Mateos-Timoneda, M.A. Biofabrication of tissue constructs by 3D bioprinting of cell-laden microcarriers. *Biofabrication* **2014**, *6*, 035020. [[CrossRef](#)]
64. Li, T.J.; Aspler, J.; Kingsland, A.; Cormier, L.M.; Zou, X.J. 3d printing—a review of technologies, markets, and opportunities for the forest industry. *J. Sci. Technol. For. Prod. Process* **2016**, *5*, 30.
65. Muñoz, J.; Pumera, M. 3D-printed biosensors for electrochemical and optical applications. *TrAC Trends Anal. Chem.* **2020**, *128*, 115933. [[CrossRef](#)]
66. Aslanzadeh, S.; Saghlatoon, H.; Honari, M.M.; Mirzavand, R.; Montemagno, C.; Mousavi, P. Investigation on electrical and mechanical properties of 3D printed nylon 6 for RF/microwave electronics applications. *Addit. Manuf.* **2018**, *21*, 69–75. [[CrossRef](#)]
67. Calignano, F.; Lorusso, M.; Roppolo, I.; Minetola, P. Investigation of the Mechanical Properties of a Carbon Fibre-Reinforced Nylon Filament for 3D Printing. *Machines* **2020**, *8*, 52. [[CrossRef](#)]
68. Farina, I.; Singh, N.; Colangelo, F.; Luciano, R.; Bonazzi, G.; Fraternali, F. High-performance nylon-6 sustainable filaments for additive manufacturing. *Materials* **2019**, *12*, 3955. [[CrossRef](#)]
69. Tambrallimath, V.; Keshavamurthy, R.; Saravanabavan, D.; Koppad, P.G.; Kumar, G.P. Thermal behavior of PC-ABS based graphene filled polymer nanocomposite synthesized by FDM process. *Compos. Commun.* **2019**, *15*, 129–134. [[CrossRef](#)]
70. Tambrallimath, V.; Keshavamurthy, R.; Saravanabavan, D.; Koppad, P.G.; Sethuram, D. Mechanical characterization of PC-ABS reinforced with CNT nanocomposites developed by fused deposition modelling. *J. Phys. Conf. Ser. IOP Publ.* **2020**, *1455*, 012003. [[CrossRef](#)]
71. Roberson, D.; Shemelya, C.M.; MacDonald, E.; Wicker, R. Expanding the applicability of FDM-type technologies through materials development. *Rapid Prototyp. J.* **2015**, *21*, 137–143. [[CrossRef](#)]
72. Park, S.J.; Lee, J.E.; Lee, H.B.; Park, J.; Lee, N.K.; Son, Y.; Park, S.H. 3D printing of bio-based polycarbonate and its potential applications in ecofriendly indoor manufacturing. *Addit. Manuf.* **2020**, *31*, 100974. [[CrossRef](#)]
73. Geng, Y.; He, H.; Liu, H. Preparation of polycarbonate/poly (lactic acid) with improved printability and processability for fused deposition modeling. *Polym. Adv. Technol.* **2020**, *31*, 2848–2862. [[CrossRef](#)]
74. Revilla-León, M.; Özcan, M. Additive manufacturing technologies used for processing polymers: Current status and potential application in prosthetic dentistry. *J. Prosthodont.* **2019**, *28*, 146–158. [[CrossRef](#)]
75. Georgopoulou, A.; Sebastian, T.; Clemens, F. Thermoplastic elastomer composite filaments for strain sensing applications extruded with a fused deposition modelling 3D printer. *Flex. Print. Electron.* **2020**, *5*, 035002. [[CrossRef](#)]
76. Haryńska, A.; Gubanska, I.; Kucinnska-Lipka, J.; Janik, H. Fabrication and characterization of flexible medical-grade TPU filament for fused deposition modeling 3DP technology. *Polymers* **2018**, *10*, 1304. [[CrossRef](#)]
77. Wang, P.; Zou, B.; Ding, S.L.; Huang, C.Z.; Shi, Z.Y.; Ma, Y.S.; Yao, P. Preparation of short CF/GF reinforced PEEK composite filaments and their comprehensive properties evaluation for FDM-3D printing. *Compos. Part B Eng.* **2020**, *198*, 108175. [[CrossRef](#)]
78. Wang, P.; Zou, B.; Xiao, H.C.; Ding, S.L.; Huang, C.Z. Effects of printing parameters of fused deposition modeling on mechanical properties, surface quality, and microstructure of PEEK. *J. Mater. Process. Technol.* **2019**, *271*, 62–74. [[CrossRef](#)]
79. Rinaldi, M.; Cecchini, F.; Pigliaru, L.; Ghidini, T.; Lumaca, F.; Nanni, F. Additive manufacturing of polyether ether ketone (PEEK) for space applications: A nanosat polymeric structure. *Polymers* **2021**, *13*, 11. [[CrossRef](#)]
80. Liu, Z.; Wang, G.; Huo, Y.; Zhao, W. Research on precise control of 3D print nozzle temperature in PEEK material. *AIP Conf. Proc.* **2017**, *1890*, 040076.
81. Haffner, M.; Quinn, A.; Hsieh, T.Y.; Strong, E.B.; Steele, T. Optimization of 3D print material for the recreation of patient-specific temporal bone models. *Ann. Otol. Rhinol. Laryngol.* **2018**, *127*, 338–343. [[CrossRef](#)] [[PubMed](#)]



82. Capel, A.J.; Rington, R.P.; Lewis, M.P.; Christie, S.D. 3D printing for chemical, pharmaceutical and biological applications. *Nat. Rev. Chem.* **2018**, *2*, 422–436. [[CrossRef](#)]
83. Redaelli, D.F.; Abbate, V.; Storm, F.A.; Ronca, A.; Sorrentino, A.; Capitani, C.D.; Biffi, E.; Ambrosio, L.; Colombo, G.; Frascini, P. 3D printing orthopedic scoliosis braces: A test comparing FDM with thermoforming. *Int. J. Adv. Manuf. Technol.* **2020**, *111*, 1707–1720. [[CrossRef](#)]
84. Subbarao, C.V.; Reddy, Y.S.; Inturi, V.; Reddy, M.I. Dynamic Mechanical Analysis of 3D Printed PETG Material. *IOP Conf. Ser. Mater. Sci. Eng.* **2021**, *1057*, 012031. [[CrossRef](#)]
85. Blanco, I.; Rapisarda, M.; Portuesi, S.; Ognibene, G.; Cicala, G. Thermal behavior of PEI/PETG blends for the application in fused deposition modelling (FDM). *AIP Conf. Proc.* **2018**, *1981*, 020181.
86. Cicala, G.; Ognibene, G.; Portuesi, S.; Blanco, I.; Rapisarda, M.; Pergolizzi, E.; Recca, G. Comparison of Ultem 9085 used in fused deposition modelling (FDM) with polyetherimide blends. *Materials* **2018**, *11*, 285. [[CrossRef](#)]
87. Zhang, X.; Chen, L. Effects of laser scanning speed on surface roughness and mechanical properties of aluminum/Poly(lactic acid) (Al/PLA) composites parts fabricated by fused deposition modeling. *Polym. Test.* **2020**, *91*, 106785. [[CrossRef](#)]
88. Zhang, X.; Chen, L.; Mulholland, T.; Osswald, T.A. Effects of raster angle on the mechanical properties of PLA and Al/PLA composite part produced by fused deposition modeling. *Polym. Adv. Technol.* **2019**, *30*, 2122–2135. [[CrossRef](#)]
89. Vardhan, H.; Kumar, R.; Chohan, J.S. Investigation of tensile properties of sprayed aluminium based PLA composites fabricated by FDM technology. *Mater. Today Proc.* **2020**, *33*, 1599–1604. [[CrossRef](#)]
90. Pavan, M.V.; Balamurugan, K.; Balamurugan, P. Compressive test Fractured Surface analysis on PLA-Cu composite filament printed at different FDM conditions. *IOP Conf. Ser. Mater. Sci. Eng.* **2020**, *988*, 012019. [[CrossRef](#)]
91. Balamurugan, K.; Pavan, M.V.; Ali, S.A.; Kalusuraman, G. Compression and flexural study on PLA-Cu composite filament using FDM. *Mater. Today Proc.* **2021**, *44*, 1687–1691. [[CrossRef](#)]
92. Gong, H.; Snelling, D.; Kardel, K.; Carrano, A. Comparison of Stainless Steel 316L Parts Made by FDM- and SLM-Based Additive Manufacturing Processes. *JOM* **2018**, *71*, 880–885. [[CrossRef](#)]
93. Daver, F.; Lee, K.P.M.; Brandt, M.; Shanks, R. Cork-PLA composite filaments for fused deposition modelling. *Compos. Sci. Technol.* **2018**, *168*, 230–237. [[CrossRef](#)]
94. da Silva, S.P.M.; Antunes, T.; Costa, M.E.V.; Oliveira, J.M. Cork-like filaments for Additive Manufacturing. *Addit. Manuf.* **2020**, *34*, 101229.
95. Le Duigou, A.; Castro, M.; Bevan, R.; Martin, N. 3D printing of wood fibre biocomposites: From mechanical to actuation functionality. *Mater. Des.* **2016**, *96*, 106–114. [[CrossRef](#)]
96. Ayrimis, N.; Kariz, M.; Kwon, J.H.; Kuzman, M.K. Effect of printing layer thickness on water absorption and mechanical properties of 3D-printed wood/PLA composite materials. *Int. J. Adv. Manuf. Technol.* **2019**, *102*, 2195–2200. [[CrossRef](#)]
97. Liu, Z.; Lei, Q.; Xing, S. Mechanical characteristics of wood, ceramic, metal and carbon fiber-based PLA composites fabricated by FDM. *J. Mater. Res. Technol.* **2019**, *8*, 3741–3751. [[CrossRef](#)]
98. Kumar, S.D.; Venkadeshwaran, K.; Aravindan, M. Fused deposition modelling of PLA reinforced with cellulose nano-crystals. *Mater. Today Proc.* **2020**, *33*, 868–875. [[CrossRef](#)]
99. Wang, Z.; Xu, J.; Lu, Y.; Ma, J.; Zhou, X. Preparation of 3D printable micro/nanocellulose-poly(lactic acid) (MNC/PLA) composite wire rods with high MNC constitution. *Ind. Crops Prod.* **2017**, *109*, 889–896. [[CrossRef](#)]
100. Zhang, Y.; Cui, L.; Xu, H.; Feng, X.; Wang, B.; Pukánszky, B. Poly(lactic acid)/cellulose nanocrystal composites via the Pickering emulsion approach: Rheological, thermal and mechanical properties. *Int. J. Biol. Macromol.* **2019**, *137*, 197–204. [[CrossRef](#)] [[PubMed](#)]
101. Zhang, X.; Shi, J.; Ye, H.; Dong, Y.; Zhou, Q. Combined effect of cellulose nanocrystals and poly (butylene succinate) on poly (lactic acid) crystallization: The role of interfacial affinity. *Carbohydr. Polym.* **2018**, *179*, 79–85. [[CrossRef](#)] [[PubMed](#)]
102. Schmitz, D.P.; Ecco, L.G.; Dul, S.; Pereira, E.C.L.; Soares, B.G.; Barra, G.M.O.; Pegoretti, A. Electromagnetic interference shielding effectiveness of ABS carbon-based composites manufactured via fused deposition modelling. *Mater. Today Commun.* **2018**, *15*, 70–80. [[CrossRef](#)]
103. Dawoud, M.; Taha, I.; Ebeid, S.J. Strain sensing behaviour of 3D printed carbon black filled ABS. *J. Manuf. Processes* **2018**, *35*, 337–342. [[CrossRef](#)]
104. Sanatgar, R.H.; Campagne, C.; Nierstrasz, V. Investigation of the adhesion properties of direct 3D printing of polymers and nanocomposites on textiles: Effect of FDM printing process parameters. *Appl. Surf. Sci.* **2017**, *403*, 551–563. [[CrossRef](#)]
105. Tirado-Garcia, I.; Garcia-Gonzalez, D.; Garzon-Hernandez, S.; Rusinek, A.; Robles, G.; Martinez-Tarifa, J.M.; Arias, A. Conductive 3D printed PLA composites: On the interplay of mechanical, electrical and thermal behaviours. *Compos. Struct.* **2021**, *265*, 113744. [[CrossRef](#)]
106. Abdalla, A.; Hamzah, H.H.; Keattch, O.; Covill, D.; Patel, B.A. Augmentation of conductive pathways in carbon black/PLA 3D-printed electrodes achieved through varying printing parameters. *Electrochim. Acta* **2020**, *354*, 136618. [[CrossRef](#)]
107. Dul, S.; Fambri, L.; Pegoretti, A. Fused deposition modelling with ABS-graphene nanocomposites. *Compos. Part A Appl. Sci. Manuf.* **2016**, *85*, 181–191. [[CrossRef](#)]
108. Sakunphokesup, K.; Kongkrenki, P.; Pongwisuthiruchte, A.; Aumnate, C.; Potiyaraj, P. Graphene-enhanced ABS for FDM 3D printing: Effects of masterbatch preparation techniques. *IOP Conf. Ser. Mater. Sci. Eng.* **2019**, *600*, 012001, IOP Publishing. [[CrossRef](#)]

109. Waheed, Q.; Khan, A.N.; Jan, R. Investigating the reinforcement effect of few layer graphene and multi-walled carbon nanotubes in acrylonitrile-butadiene-styrene. *Polymer* **2016**, *97*, 496–503. [[CrossRef](#)]
110. Singh, R.; Sandhu, G.S.; Penna, R.; Farina, I. Investigations for thermal and electrical conductivity of ABS-graphene blended prototypes. *Materials* **2017**, *10*, 881. [[CrossRef](#)] [[PubMed](#)]
111. Tambrallimath, V.; Keshavamurthy, R.; Saravanbavan, D.; Kumar, G.P.; Kumar, M.H. Synthesis and characterization of graphene filled PC-ABS filament for FDM applications. *AIP Conf. Proc.* **2019**, *2057*, 020039, AIP Publishing LLC.
112. Wang, F.; Zhang, Y.; Zhang, B.B.; Hong, R.Y.; Kumar, M.R.; Xie, C.R. Enhanced electrical conductivity and mechanical properties of ABS/EPDM composites filled with graphene. *Compos. Part B Eng.* **2015**, *83*, 66–74. [[CrossRef](#)]
113. Jyoti, J.; Basu, S.; Singh, B.P.; Dhakate, S.R. Superior mechanical and electrical properties of multiwall carbon nanotube reinforced acrylonitrile butadiene styrene high performance composites. *Compos. Part B Eng.* **2015**, *83*, 58–65. [[CrossRef](#)]
114. Rodríguez-Vidal, E.; Quintana, I.; Gadea, C. Laser transmission welding of ABS: Effect of CNTs concentration and process parameters on material integrity and weld formation. *Opt. Laser Technol.* **2014**, *57*, 194–201. [[CrossRef](#)]
115. Sanatgar, R.H.; Cayla, A.; Campagne, C.; Nierstrasz, V. Morphological and electrical characterization of conductive polylactic acid based nanocomposite before and after FDM 3D printing. *J. Appl. Polym. Sci.* **2019**, *136*, 47040. [[CrossRef](#)]
116. Shao, S.; Zhou, S.; Li, L.; Li, J.; Luo, C.; Wang, J.; Li, X.; Weng, J. Osteoblast function on electrically conductive electrospun PLA/MWCNTs nanofibers. *Biomaterials* **2011**, *32*, 2821–2833. [[CrossRef](#)]
117. Wu, D.; Spanou, A.; Diez-Escudero, A.; Persson, C. 3D-printed PLA/HA composite structures as synthetic trabecular bone: A feasibility study using fused deposition modeling. *J. Mech. Behav. Biomed. Mater.* **2020**, *103*, 103608. [[CrossRef](#)]
118. Corcione, C.E.; Gervaso, F.; Scalera, F.; Montagna, F.; Maiullaro, T.; Sannino, A.; Maffezzoli, A. 3D printing of hydroxyapatite polymer-based composites for bone tissue engineering. *J. Polym. Eng.* **2017**, *37*, 741–746. [[CrossRef](#)]
119. Pierantozzi, D.; Scalzone, A.; Jindal, S.; Stipniece, L.; Salma-Ancane, K.; Dalgano, K.; Gentile, P.; Mancuso, E. 3D printed Sr-containing composite scaffolds: Effect of structural design and material formulation towards new strategies for bone tissue engineering. *Compos. Sci. Technol.* **2020**, *19*, 108069. [[CrossRef](#)]
120. Zhao, J.; Guo, L.Y.; Yang, X.B.; Weng, J. Preparation of bioactive porous HA/PCL composite scaffolds. *Appl. Surf. Sci.* **2008**, *255*, 2942–2946. [[CrossRef](#)]
121. Heo, S.J.; Kim, S.E.; Wei, J.; Hyun, Y.T.; Yun, H.S.; Kim, D.H.; Shin, J.W.; Shin, J.W. Fabrication and characterization of novel nano-and micro-HA/PCL composite scaffolds using a modified rapid prototyping process. *J. Biomed. Mater. Res. Part A Off. J. Soc. Biomater. Jpn. Soc. Biomater. Aust. Soc. Biomater. Korean Soc. Biomater.* **2009**, *89*, 108–116. [[CrossRef](#)]
122. Manzoor, F.; Golbang, A.; Jindal, S.; Dixon, D.; McIlhagger, A.; Harkin-Jones, E.; Crawford, D.; Mancuso, E. 3D printed PEEK/HA composites for bone tissue engineering applications: Effect of material formulation on mechanical performance and bioactive potential. *J. Mech. Behav. Biomed. Mater.* **2021**, *121*, 104601. [[CrossRef](#)] [[PubMed](#)]
123. Sang, L.; Han, S.; Li, Z.; Yang, X.; Hou, W. Development of short basalt fiber reinforced polylactide composites and their feasible evaluation for 3D printing applications. *Compos. Part B Eng.* **2019**, *164*, 629–639. [[CrossRef](#)]
124. Nagendra, J.; Prasad, M.G.; Shashank, S.; Vijay, N.; Ali, S.M.; Suresh, V. Nylon-aramid polymer composite as sliding liner for lube-less sliding bearing by fused deposition modeling. *AIP Conf. Proc.* **2019**, *2057*, 020047.
125. Le Duigou, A.; Barbe, A.; Guilou, E.; Castro, M. 3D printing of continuous flax fibre reinforced biocomposites for structural applications. *Mater. Des.* **2019**, *180*, 107884. [[CrossRef](#)]
126. Bilkar, D.; Keshavamurthy, R.; Tambrallimath, V. Influence of carbon nanofiber reinforcement on mechanical properties of polymer composites developed by FDM. *Mater. Today Proc.* **2021**, *46*, 4559–4562. [[CrossRef](#)]
127. Ning, F.; Cong, W.L.; Qiu, J.J.; Wei, J.H.; Wang, S.R. Additive manufacturing of carbon fiber reinforced thermoplastic composites using fused deposition modeling. *Compos. Part B Eng.* **2015**, *80*, 369–378. [[CrossRef](#)]
128. Yu, N.; Sun, X.Y.; Wang, Z.; Zhang, D.J.; Li, J. Effects of auxiliary heat on warpage and mechanical properties in carbon fiber/ABS composite manufactured by fused deposition modeling. *Mater. Des.* **2020**, *195*, 108978. [[CrossRef](#)]
129. Tandon, S.; Kacker, R.; Sudhakar, K. Experimental investigation on tensile properties of the polymer and composite specimens printed in a Triangular pattern. *J. Manuf. Process.* **2021**, *68*, 706–715. [[CrossRef](#)]
130. Yu, Y.; Liu, H.L.; Qian, K.R.; Yang, H.; McGehee, M.; Gu, J.Z.; Luo, D.L.; Yao, L.N.; Zhang, Y.J. Material characterization and precise finite element analysis of fiber reinforced thermoplastic composites for 4D printing. *Comput.-Aided Des.* **2020**, *122*, 102817. [[CrossRef](#)]
131. Gavali, V.C.; Kubade, P.R.; Kulkarni, H.B. Mechanical and thermo-mechanical properties of carbon fiber reinforced thermoplastic composite fabricated using fused deposition modeling method. *Mater. Today Proc.* **2020**, *22*, 1786–1795. [[CrossRef](#)]
132. Kamaal, M.; Anas, M.; Rastogi, H.; Bhardwaj, N.; Rahaman, A. Effect of FDM process parameters on mechanical properties of 3D-printed carbon fibre-PLA composite. *Prog. Addit. Manuf.* **2021**, *6*, 63–69. [[CrossRef](#)]
133. Lin, L.; Schlarb, A.K. Recycled carbon fibers as reinforcements for hybrid PEEK composites with excellent friction and wear performance. *Wear* **2019**, *432*, 202928. [[CrossRef](#)]
134. Stepashkin, A.; Chukov, D.I.; Senatov, F.S.; Salimon, A.I.; Korsunsky, A.M.; Kaloshkin, S.D. 3D-printed PEEK-carbon fiber (CF) composites: Structure and thermal properties. *Compos. Sci. Technol.* **2018**, *164*, 319–326. [[CrossRef](#)]
135. Huang, H.; Liu, W.; Liu, Z. An additive manufacturing-based approach for carbon fiber reinforced polymer recycling. *CIRP Ann.* **2020**, *69*, 33–36. [[CrossRef](#)]

136. Prajapati, A.R.; Dave, H.K.; Raval, H.K. An Experimental Study on Mechanical, Thermal and Flame-Retardant Properties of 3D-Printed Glass-Fiber-Reinforced Polymer Composites. *J. Mater. Eng. Perform.* **2021**, *30*, 5266–5277. [[CrossRef](#)]
137. Caminero, M.; Chacon, J.M.; Gracia-Moreno, I.; Rodriguez, G.P. Impact damage resistance of 3D printed continuous fibre reinforced thermoplastic composites using fused deposition modelling. *Compos. Part B Eng.* **2018**, *148*, 93–103. [[CrossRef](#)]
138. Dickson, A.N.; Barry, J.N.; McDonnell, K.A.; Dowling, D.P. Fabrication of continuous carbon, glass and Kevlar fibre reinforced polymer composites using additive manufacturing. *Addit. Manuf.* **2017**, *16*, 146–152. [[CrossRef](#)]
139. de Toro, E.V.; Sobrino, J.C.; Martinez, A.M.; Eguia, V.M. Analysis of the influence of the variables of the Fused Deposition Modeling (FDM) process on the mechanical properties of a carbon fiber-reinforced polyamide. *Procedia Manuf.* **2019**, *41*, 731–738. [[CrossRef](#)]
140. Barrios, J.M.; Romero, P.E. Improvement of Surface Roughness and Hydrophobicity in PETG Parts Manufactured via Fused Deposition Modeling (FDM): An Application in 3D Printed Self-Cleaning Parts. *Materials* **2019**, *12*, 2499. [[CrossRef](#)] [[PubMed](#)]
141. Zharylkassyn, B.; Perveen, A.; Talamona, D. Effect of process parameters and materials on the dimensional accuracy of FDM parts. *Mater. Today Proc.* **2020**, *44*, 1307–1311. [[CrossRef](#)]
142. Nancharaiyah, T.; Raju, D.R.; Raju, V.R. An experimental investigation on surface quality and dimensional accuracy of FDM components. *Int. J. Emerg. Technol.* **2010**, *1*, 106–111.
143. Dey, A.; Yodo, N. A Systematic Survey of FDM Process Parameter Optimization and Their Influence on Part Characteristics. *J. Manuf. Mater. Process.* **2019**, *3*, 64. [[CrossRef](#)]
144. Wang, T.M.; Xi, J.T.; Jin, Y. A model research for prototype warp deformation in the FDM process. *Int. J. Adv. Manuf. Technol.* **2007**, *33*, 1087–1096. [[CrossRef](#)]
145. van Manen, T.; Janbaz, S.; Zadpoor, A.A. Programming the shape-shifting of flat soft matter. *Mater. Today* **2018**, *21*, 144–163. [[CrossRef](#)]
146. Redwood, B.; Schöffner, F.; Garret, B. *The 3D Printing Handbook: Technologies, Design and Applications*; 3D Hubs: Amsterdam, The Netherlands, 2017.
147. Kaur, G.; Singari, R.M.; Kumar, H. A review of fused filament fabrication (FFF): Process parameters and their impact on the tribological behavior of polymers (ABS). *Mater. Today Proc.* **2021**, *51*, 854–860. [[CrossRef](#)]
148. Afrose, M.F.; Masood, S.H.; Ioveniti, P.; Nikzad, M.; Sbarski, I. Effects of part build orientations on fatigue behaviour of FDM-processed PLA material. *Prog. Addit. Manuf.* **2016**, *1*, 21–28. [[CrossRef](#)]
149. Patil, H.; Tiwari, R.V.; Repka, M.A. Hot-melt extrusion: From theory to application in pharmaceutical formulation. *AAPS PharmSciTech* **2016**, *17*, 20–42. [[CrossRef](#)]
150. Gaspar-Cunha, A.; Covas, J.A.; Costa, M.; Fernanda, P.; Costa, L. *Optimization of Single Screw Extrusion*; Technicka Univerzita Kosice: Košice, Slovakia, 2018.
151. Maniruzzaman, M.; Boateng, J.S.; Snowden, M.J.; Douroumis, D. A review of hot-melt extrusion: Process technology to pharmaceutical products. *Int. Sch. Res. Not.* **2012**, *2012*, 436763. [[CrossRef](#)] [[PubMed](#)]
152. Singhal, S.; Lohar, V.K.; Arora, V. Hot Melt Extrusion Technique. *Webmedcentral Pharm. Sci.* **2011**, *2*, 1.
153. Chokshi, R.; Zia, H. Hot-melt extrusion technique: A review. *Iran. J. Pharm. Res.* **2004**, *3*, 3–16.
154. Censi, R.; Gigliobianco, M.R.; Casadidio, C. Hot Melt Extrusion: Highlighting Physicochemical Factors to Be Investigated While Designing and Optimizing a Hot Melt Extrusion Process. *Pharmaceutics* **2018**, *10*, 89. [[CrossRef](#)] [[PubMed](#)]
155. Abeykoon, C. *Polymer Extrusion: A Study on Thermal Monitoring Techniques and Melting Issues*, 1st ed.; LAP LAMBERT Academic Publishing: Berlin, Germany, 2012.
156. Wilczyński, K.J.; Lewandowski, A.; Nastaj, A.; Wilczyński, K. Modeling for Starve Fed/Flood Fed Mixing Single-Screw Extruders. *Int. Polym. Process.* **2016**, *31*, 82–91. [[CrossRef](#)]
157. Repka, M.A.; Langley, N.; DiNunzio, J. *Melt Extrusion: Materials, Technology and Drug Product Design*; Springer Science & Business Media: New York, NY, USA, 2013; Volume 9.
158. Geus, H.G. Developments in manufacturing techniques for technical nonwovens. In *Advances in Technical Nonwovens*; Woodhead Publishing: Sawston, UK, 2016; pp. 133–153.
159. Wilczyński, K.; Nastaj, A.; Wilczyński, K.J. Melting Model for Starve Fed Single Screw Extrusion of Thermoplastics. *Int. Polym. Process.* **2013**, *28*, 34–42. [[CrossRef](#)]
160. Wilczyński, K.; Lewandowski, A.; Wilczyński, K.J. Experimental study for starve-fed single screw extrusion of thermoplastics. *Polym. Eng. Sci.* **2012**, *52*, 1258–1270. [[CrossRef](#)]
161. Tan, D.K.; Maniruzzaman, M.; Nokhodchi, A. Advanced Pharmaceutical Applications of Hot-Melt Extrusion Coupled with Fused Deposition Modelling (FDM) 3D Printing for Personalised Drug Delivery. *Pharmaceutics* **2018**, *10*, 203. [[CrossRef](#)]
162. Wilczynski, K.; White, J.L. Melting Model for Intermeshing Counter-Rotating Twin-Screw Extruders. *Polym. Eng. Sci.* **2003**, *43*, 1715–1726. [[CrossRef](#)]
163. Bouvier, J.M.; Campanella, O.H. *Extrusion Processing Technology: Food and Non-Food Biomaterials*; John Wiley & Sons: Hoboken, NJ, USA, 2014.
164. Tadmor, Z.; Gogos, C.G. *Principles of Polymer Processing*; John Wiley & Sons: Hoboken, NJ, USA, 2013.
165. Crowley, M.M.; Zhang, F.; Repka, M.A.; Thumma, S.; Upadhye, S.B.; Battu, S.K.; McGinity, J.W.; Martin, C. Pharmaceutical Applications of Hot-Melt Extrusion: Part I. *Drug Dev. Ind. Pharm.* **2007**, *33*, 909–926. [[CrossRef](#)]



166. Wilczyński, K.; Lewandowski, A.; Wilczynski, K.J. Experimental study of melting of LDPE/PS polyblend in an intermeshing counter-rotating twin screw extruder. *Polym. Eng. Sci.* **2012**, *52*, 449–458. [[CrossRef](#)]
167. Wilson, M.; Williams, M.A.; Jones, D.S.; Andrews, G.P. Hot-melt extrusion technology and pharmaceutical application. *Ther. Deliv.* **2012**, *3*, 787–797. [[CrossRef](#)] [[PubMed](#)]
168. Uitterhaegen, E.; Evon, P. Twin-screw extrusion technology for vegetable oil extraction: A review. *J. Food Eng.* **2017**, *212*, 190–200. [[CrossRef](#)]
169. Singh, R.; Singh, S. Development of nylon based FDM filament for rapid tooling application. *J. Institution Eng.* **2014**, *95*, 103–108. [[CrossRef](#)]
170. Osman, M.A.; Atia, M.R.A. Investigation of ABS-rice straw composite feedstock filament for FDM. *Rapid Prototyp. J.* **2018**, *24*, 6. [[CrossRef](#)]
171. Weng, Z.; Wang, J.; Senthil, T.; Wu, L. Mechanical and thermal properties of ABS/montmorillonite nanocomposites for fused deposition modeling 3D printing. *Mater. Des.* **2016**, *102*, 276–283. [[CrossRef](#)]
172. Boparai, K.S.; Singh, R.; Singh, H. Experimental investigations for development of Nylon6-Al-Al<sub>2</sub>O<sub>3</sub> alternative FDM filament. *Rapid Prototyp. J.* **2016**, *22*, 2. [[CrossRef](#)]
173. Melocchi, A.; Parietti, F.; Loreti, G.; Maroni, A.; Gazzaniga, A.; Zema, L. 3D printing by fused deposition modeling (FDM) of a swellable/erodible capsular device for oral pulsatile release of drugs. *J. Drug Deliv. Sci. Technol.* **2015**, *30*, 360–367. [[CrossRef](#)]
174. Sezer, H.K.; Eren, O. FDM 3D printing of MWCNT re-inforced ABS nano-composite parts with enhanced mechanical and electrical properties. *J. Manuf. Processes* **2019**, *37*, 339–347. [[CrossRef](#)]
175. Kuo, C.C.; Liu, L.C.; Teng, W.F.; Chang, H.Y.; Cchien, F.M.; Liao, S.J.; Kuo, W.F.; Chen, C.M. Preparation of starch/acrylonitrile-butadiene-styrene copolymers (ABS) biomass alloys and their feasible evaluation for 3D printing applications. *Compos. Part B Eng.* **2016**, *86*, 36–39. [[CrossRef](#)]
176. Ahn, S.H.; Montero, M.; Odell, D.; Roundy, S.; Wright, P.K. Anisotropic material properties of fused deposition modeling ABS. *Rapid Prototyp. J.* **2002**, *8*, 4. [[CrossRef](#)]
177. Nabipour, M.; Akhoundi, B.; Saed, A.B. Manufacturing of polymer/metal composites by fused deposition modeling process with polyethylene. *J. Appl. Polym. Sci.* **2020**, *137*, 48717. [[CrossRef](#)]
178. Mogan, J.; Sandanamsamy, L.; Halim, N.A.; Kadirgama, K.; Ramasamy, D. A review of FDM and graphene-based polymer composite. *IOP Conf. Ser. Mater. Sci. Eng.* **2021**, *1078*, 012032. [[CrossRef](#)]
179. Abadi, A.H.; Thai, H.T.; Cole, V.P.; Patel, V.I. Elastic properties of 3D printed fibre-reinforced structures. *Compos. Struct.* **2018**, *193*, 8–18. [[CrossRef](#)]
180. Gray, R.W.; Baird, D.G.; Bohn, J.H. Effects of processing conditions on short TLCP fiber reinforced FDM parts. *Rapid Prototyp. J.* **1998**, *4*, 1. [[CrossRef](#)]
181. Li, Y.; Gao, S.; Dong, G.; Ding, X.; Duan, X. Additive manufacturing of PLA and CF/PLA binding layer specimens via fused deposition modeling. *J. Mater. Eng. Perform.* **2018**, *27*, 492–500. [[CrossRef](#)]
182. Kuan, C.F.; Kuan, H.C.; Ma, C.C.M.; Chen, C.H. Mechanical and electrical properties of multi-wall carbon nanotube/poly (lactic acid) composites. *J. Phys. Chem. Solids* **2008**, *69*, 1395–1398. [[CrossRef](#)]
183. Li, N.; Li, Y.; Liu, S. Rapid prototyping of continuous carbon fiber reinforced polylactic acid composites by 3D printing. *J. Mater. Process. Technol.* **2016**, *238*, 218–225. [[CrossRef](#)]
184. Liu, Z. Review and Prospect of Thermal Analysis Technology Applied to Study Thermal Properties of Energetic Materials. *FirePhysChem* **2021**, *1*, 129–138. [[CrossRef](#)]
185. Qian, H.; Kai, W.; Hongde, X.; Li, Z.; Penghui, Y. Investigation on foaming and secondary reactions with a novel visual equipment and impacts on thermal analysis. *Thermochim. Acta* **2021**, *703*, 179014. [[CrossRef](#)]
186. Kim, S.J.; Lee, J.C.; Ko, J.K.; Lee, S.H.; Kim, N.A.; Jeong, S.H. 3D-printed tablets using a single-step hot-melt pneumatic process for poorly soluble drugs. *Int. J. Pharm.* **2021**, *595*, 120257. [[CrossRef](#)] [[PubMed](#)]
187. Goyanes, A.; Buanz, A.B.M.; Hatton, G.B.; Gaisford, S.; Basit, A.W. 3D printing of modified-release aminosalicylate (4-ASA and 5-ASA) tablets. *Eur. J. Pharm. Biopharm.* **2015**, *89*, 157–162. [[CrossRef](#)] [[PubMed](#)]
188. Gioumouxouzis, C.I.; Katsamenis, O.L.; Bouropoulos, N.; Fatouros, D.G. 3D printed oral solid dosage forms containing hydrochlorothiazide for controlled drug delivery. *J. Drug Deliv. Sci. Technol.* **2017**, *40*, 164–171. [[CrossRef](#)]
189. Lin, C.P.; Chang, Y.M.; Gupta, J.P.; Shu, C.M. Comparisons of TGA and DSC approaches to evaluate nitrocellulose thermal degradation energy and stabilizer efficiencies. *Process Saf. Environ. Prot.* **2010**, *88*, 413–419. [[CrossRef](#)]
190. Olam, M.; Tosun, N. 3D-printed polylactide/hydroxyapatite/titania composite filaments. *Mater. Chem. Phys.* **2022**, *276*, 125267. [[CrossRef](#)]
191. Eleftheriadis, G.K.; Ritzoulis, C.; Bbouropoulos, N.; Tzetzis, D.; Andreadis, D.A.; Boetker, J.; Rantanen, J.; Fatouros, D.G. Unidirectional drug release from 3D printed mucoadhesive buccal films using FDM technology: In vitro and ex vivo evaluation. *Eur. J. Pharm. Biopharm.* **2019**, *144*, 180–192. [[CrossRef](#)]
192. Foerster, A.; Annarasa, V.; Terry, A.; Wildman, R.; Hague, R.; Irvine, D.; Focatiis, D.S.A.D.; Tuck, C. UV-curable silicone materials with tuneable mechanical properties for 3D printing. *Mater. Des.* **2021**, *205*, 109681. [[CrossRef](#)]
193. Real, J.P.; Barberis, M.E.; Camacho, N.M.; Bruni, S.S.; Palma, S.D. Design of novel oral ricobendazole formulation applying melting solidification printing process (MESO-PP): An innovative solvent-free alternative method for 3D printing using a simplified concept and low temperature. *Int. J. Pharm.* **2020**, *587*, 119653. [[CrossRef](#)]

194. What Is the Difference between Thermogravimetric Analysis (TGA) and Differential Scanning Calorimetry (DSC). Available online: <https://www.particletechlabs.com/ptl-press/what-is-the-difference-between-thermogravimetric-analysis-tga-and-differential-scanning-calorimetry-dsc> (accessed on 17 October 2022).
195. Sadhasivam, B.; Ramamoorthy, D.; Dhamodharan, R. Scale-up of non-toxic poly(butylene adipate-co-terephthalate)-Chitin based nanocomposite articles by injection moulding and 3D printing. *Int. J. Biol. Macromol.* **2020**, *165*, 3145–3155. [CrossRef]
196. Biswas, M.C.; Tiimob, B.J.; Abdela, W.; Jeelani, S.; Rangari, V.K. Nano silica-carbon-silver ternary hybrid induced antimicrobial composite films for food packaging application. *Food Packag. Shelf Life* **2019**, *19*, 104–113. [CrossRef]
197. Biswas, M.C.; Jeelani, S.; Rangari, V. Influence of biobased silica/carbon hybrid nanoparticles on thermal and mechanical properties of biodegradable polymer films. *Compos. Commun.* **2017**, *4*, 43–53. [CrossRef]
198. Sarwar, Z.; Yousef, S.; Tatariants, M.; Krugly, E.; Cruzas, D.; Danilovas, P.P.; Baltusnikas, A.; Martuzevicius, D. Fibrous PEBA-graphene nanocomposite filaments and membranes fabricated by extrusion and additive manufacturing. *Eur. Polym. J.* **2019**, *121*, 109317. [CrossRef]
199. Wickramasinghe, K.C.; Sasahara, H.; Rahim, E.A.; Perera, G.I.P. Recent advances on high performance machining of aerospace materials and composites using vegetable oil-based metal working fluids. *J. Clean. Prod.* **2021**, *310*, 127459. [CrossRef]
200. Mohanavel, V.; Ali, K.S.A.; Ranganathan, K.; Jeffrey, J.A.; Ravikumar, M.M.; Rajkumar, S. The roles and applications of additive manufacturing in the aerospace and automobile sector. *Mater. Today Proc.* **2021**, *47*, 405–409. [CrossRef]
201. Altuparmak, S.C.; Xiao, B. A market assessment of additive manufacturing potential for the aerospace industry. *J. Manuf. Processes* **2021**, *68*, 728–738. [CrossRef]
202. World's First Jet-Powered, 3D Printed UAV Tops 150 mph with Lightweight Stratasys Materials. Available online: <https://www.stratasys.com/en/resources/blog/aurora-uav-3d-printing/> (accessed on 17 October 2022).
203. Gao, X.; Yu, N.; Li, J. Influence of printing parameters and filament quality on structure and properties of polymer composite components used in the fields of automotive. In *Structure and Properties of Additive Manufactured Polymer Components*; Woodhead Publishing: Sawston, UK, 2020; pp. 303–330.
204. Singh, D.; Singh, R.; Booparai, K.S.; Farina, I.; Feo, L.; Verma, A.K. In-vitro studies of SS 316 L biomedical implants prepared by FDM, vapor smoothing and investment casting. *Compos. Part B Eng.* **2018**, *132*, 107–114. [CrossRef]
205. Shanmugam, V.; Das, O.; Babu, K.; Marimuthu, U.; Veerasimman, A.; Johnson, D.J.; Neisiany, R.E.; Hedenqvist, M.S.; Ramakrishna, S.; Berto, F. Fatigue behaviour of FDM-3D printed polymers, polymeric composites and architected cellular materials. *Int. J. Fatigue* **2021**, *143*, 106007. [CrossRef]
206. Gu, P.; Li, L. Fabrication of Biomedical Prototypes with Locally Controlled Properties Using FDM. *CIRP Ann.* **2002**, *51*, 181–184. [CrossRef]
207. Melnikova, R.; Ehrmann, A.; Finsterbusch, K. 3D printing of textile-based structures by Fused Deposition Modelling (FDM) with different polymer materials. *IOP Conf. Ser. Mater. Sci. Eng.* **2014**, *62*, 012018. [CrossRef]
208. Pei, E.; Shen, J.; Watling, J. Direct 3D printing of polymers onto textiles: Experimental studies and applications. *Rapid Prototyp. J.* **2015**, *21*, 5. [CrossRef]
209. Korger, M.; Bergschneider, J.; Lutz, M.; Mahltig, B.; Finsterbusch, K.; Rabe, M. Possible applications of 3D printing technology on textile substrates. *IOP Conf. Ser. Mater. Sci. Eng.* **2016**, *141*, 012011. [CrossRef]
210. Ligon, S.C.; Liska, R.; Stampfi, J.; Gurr, M.; Mulhaupt, R. Polymers for 3D printing and customized additive manufacturing. *Chem. Rev.* **2017**, *117*, 10212–10290. [CrossRef] [PubMed]
211. Sabantina, L.; Kinzel, F.; Ehrmann, A.; Finsterbusch, K. Combining 3D printed forms with textile structures-mechanical and geometrical properties of multi-material systems. *IOP Conf. Ser. Mater. Sci. Eng.* **2015**, *87*, 012005. [CrossRef]
212. Chakraborty, S.; Biswas, M.C. 3D printing technology of polymer-fiber composites in textile and fashion industry: A potential roadmap of concept to consumer. *Compos. Struct.* **2020**, *248*, 112562. [CrossRef]
213. Chen, Y.; Ye, L.; Han, X. Experimental and numerical investigation of zero Poisson's ratio structures achieved by topological design and 3D printing of SCF/PA. *Compos. Struct.* **2022**, *293*, 115717. [CrossRef]
214. Chen, Y.; Ye, L. Designing and tailoring effective elastic modulus and negative Poisson's ratio with continuous carbon fibres using 3D printing. *Compos. Part A Appl. Sci. Manuf.* **2021**, *150*, 106625. [CrossRef]
215. Chen, Y.; Ye, L.; Kinloch, A.J.; Zhang, Y.X. 3D printed carbon-fibre reinforced composite lattice structures with good thermal-dimensional stability. *Compos. Sci. Technol.* **2022**, *227*, 109599. [CrossRef]
216. Hu, C.; Dong, J.; Luo, J.; Qin, Q.H.; Sun, G.Y. 3D printing of chiral carbon fiber reinforced polylactic acid composites with negative Poisson's ratios. *Compos. Part B Eng.* **2020**, *201*, 108400. [CrossRef]
217. Chen, Y.; Ye, L.; Zhang, Y.X.; Fu, K. Compression behaviours of 3D-printed CF/PA metamaterials: Experiment and modelling. *Int. J. Mech. Sci.* **2021**, *206*, 106634. [CrossRef]

**Disclaimer/Publisher's Note:** The statements, opinions and data contained in all publications are solely those of the individual author(s) and contributor(s) and not of MDPI and/or the editor(s). MDPI and/or the editor(s) disclaim responsibility for any injury to people or property resulting from any ideas, methods, instructions or products referred to in the content.